Tolerable Strains for HMA Overlays over Concrete Pavements

By

Ashwani Gautam

Submitted to the graduate degree program in Civil Engineering and the Graduate Faculty of the University of Kansas School of Engineering in partial fulfillment of the requirements for the degree of Master of Science.

_____
Dr. Jie Han, Chairperson

Committee members

_____
Dr. Anil Misra

_____
Dr. Robert L. Parsons

Date defended: 04/23/09

The Thesis Committee for Ashwani Gautam certifies

That this is the approved version of the following thesis:

Tolerable Strains for HMA Overlays over Concrete Pavements

Committee:

_____
Dr. Jie Han, Chairperson

_____
Dr. Anil Misra

_____
Dr. Robert L. Parsons

Date approved: 06/16/09

Acknowledgement

First and foremost I would like to express my gratefulness to my advisor Dr. Jie Han for providing me an opportunity to work in this interesting project and for his continuous encouragement and valuable suggestions throughout this research project. I would like to thank Dr. Anil Misra and Dr. Robert L. Parsons too for their support and time serving as my Master's committee members.

I received great cooperation and help from Prof. Baoshan Huang at the University of Tennessee for allowing us to use their equipments for semi-circular bend tests. I would also like to thank people from KDOT for their supply of materials and their help in preparing HMA samples for semi-circular bend tests. This project would not have come to this stage without great technical support from our lab supervisor Jim Weaver. I express my special thanks to all of them.

I would also like to thank all of my fellow classmates in KU geotechnical society who always helped and supported me when I needed. All my other friends who encouraged me continuously and provided me moral support also deserve my thanks.

Finally, I would like to express my emotional gratitude to my parents back home in India for all the support, understanding, and encouragement they have provided to me.

Table of Contents

List of tables

List of figures

Abstract

Materials from two Kansas Department of Transportation (KDOT) projects', namely 089 C-4318-01 (Mix 1) and 56-29 KA-1087-01 (Mix 2), were used for the laboratory study. Considering typical overlay thicknesses used in Kansas, samples of thickness 1.5in and 2in were chosen. Direct shear box tests and semi-circular bend tests were conducted on these chosen HMA mixtures to characterize their shear and tensile properties respectively. Crack width was simulated in lab by steel bars having thickness 0.25in, 0.375in, and 0.5in in direct shear tests. Measured relative movements of these HMA mixtures at failure varied from 4.5 percent to 9.4 percent of the sample thickness depending upon the simulated crack width. Tolerable tensile strain of Mix 1 under fatigue loading in semi-circular bend tests was 3.5 percent and that of Mix 2 was 1.4 percent for 2in thick samples. Two inch thick samples gave more consistent results than 1.5 in. thick samples hence the results obtained from 2in thick samples should be used.

1 INTRODUCTION

1.1. Problem Background

Hot-mix asphalt (HMA) overlays often prematurely exhibit a cracking pattern similar to that which existed in the old, underlying pavement. The cracking in new overlays is due to inability of the overlays to endure tensile and shear stresses. Tensile and shear stresses develop because of movement of cracked slabs of underlying old pavements concentrated around preexisting cracks. This movement is caused by combination of traffic loading (differential deflections at cracks), and expansion and contraction of existing pavements due to change in temperature or moisture change. Such movement induces shear and tensile stresses in the new overlay. When these induced tensile and shear stresses become higher than tensile and shear strengths of HMA, cracks develop in the new overlay. This phenomenon of propagation of existing cracks from old existing pavements to new overlays is called *reflective cracking*.

1.2. Problem Statement

Due to temperature and/or moisture changes, loss of subgrade support by erosion, and traffic loading, concrete pavements can develop different types of distresses during their service life. Hot Mix Asphalt (HMA) overlays are commonly used to improve the serviceability of damaged concrete pavements.

The most challenging issue for HMA overlays over concrete pavements is the development of reflection cracks through the overlays at the locations of joints and existing cracks on concrete pavements. Even though different techniques have been used to overcome this issue, they often do not provide satisfactory results and performance. Cracking of HMA overlays results from intolerable tensile and/or shear trains developed in overlays due to the movement of concrete pavements. Past research has been focused on tensile strengths, rutting, and fatigue behavior of HMA, however, very limited studies have been conducted to determine tolerable tensile and shear strains of HMA at various temperatures, overlay thicknesses, HMA mixes, and loading rates. If the strain the HMA can endure is known, methods that will limit or prevent that strain can be sought. This research is to experimentally determine the tolerable tensile and shear strains of HMA at the University of Kansas.

1.3. Objective

The main objective of this study is to experimentally determine the tolerable strain in asphalt mix under proper stimulation of field conditions for reflective cracking. Results from this experiment may be used to design HMA overlays on concrete pavements.

Direct shear box and semi-circular bend tests were conducted on selected mixes from KDOT to determine the tolerable shear and tensile strength and strain of HMA respectively. Tolerable shear strength is defined as the maximum shear

force the specimen can carry. Tolerable tensile strength is defined as the tensile strength of the HMA when the first crack starts to appear. The tolerable tensile strain is the strain corresponding to the tolerable tensile strength. Direct shear box tests can give the maximum shear force HMA can endure before failure. Static and cyclic semi-circular bend tests can be used to determine the tensile strength and strain and the fatigue behavior.

1.4. Organization

This thesis contains five chapters:

Chapter 1 presents the statement of the problem, the objective of the research, and the organization of the thesis.

Chapter 2 provides a literature review of the mechanisms of reflection cracking in hot mix asphalt overlays, the state of the research to evaluate the HMA overlays, and the techniques to minimize reflection cracking.

Chapter 3 documents the experimental study carried on for the present research, which includes the use of the equipment, the material characterization, the preparation of the samples, and the test procedures.

Chapter 4 presents the test results obtained from the experimental study of direct shear box and semi-circular bend tests for HMA samples

Chapter 5 summarizes the test results and makes conclusions and recommendations based on this research.

Data of the direct shear box tests and semi-circular bend tests are presented in Appendix at the end of this thesis.

2. LITERATURE REVIEW

2.1. Introduction

Using Hot Mix Asphalt (HMA) for rehabilitation of aged joint concrete pavements or asphalt pavements is problematic and susceptible to reflection cracking. Reflection cracking is one of the most important factors causing premature failure of HMA overlays and hence the pavements. Reflection cracking has been studied for a long time, but it is still occurring and costing millions of dollars per year. Reflection cracking is generally defined as propagation of an exiting crack pattern from existing pavements to new HMA overlays. Occurrence of reflection cracks has caused significant maintenance and serviceability issues.

Many studies (Lee et al. 2007; Abd et al. 2007; Kim et al. 2003) have been undertaken to understand and prevent reflection cracking. Currently various methods exist to minimize reflection cracking but they often lack in providing satisfactory results. Study of reflection cracking has been approached from different angles including numerical modeling, mechanistic models, field studies, and laboratory studies.

Reflection cracking occurs in new HMA overlays because of their inability to withstand tensile and shear stresses created by vertical and horizontal movements of cracked pavements underneath. This research is to experimentally determine the maximum shear and tensile strengths and strain HMA can withstand. When tolerable tensile and shear and tensile strengths and strain of HMA are known, methods can be sought to minimize or prevent the reflection cracking.

2.2. Mechanisms of Reflection Cracking

The basic mechanisms that are normally assumed to cause reflection cracking are vertical and horizontal movements of the pavement. The vertical movement of the pavement is mainly caused by moving traffic. The vertical movement in the HMA overlay is generally induced by differential movements of the underlying pavement. The horizontal movement of cracks and joints is caused by temperature changes and/or moisture changes. The vertical movement in the

overlay induces a shear stress in the HMA. The horizontal movement of cracked slabs causes high tensile stresses and strains at the bottom of the asphalt overlay and results in reflection cracking. Because at low temperature asphalt concrete is stiff, brittle and it can not withstand large temperature-induced stresses. In addition to temperature changes in underlying cracked slabs, the total movement of the cracked slab is attributed to moisture changes, slab length, and stiffness properties of the overlaying material (Sherman et al. 1982).

Lee et al. (2007) illustrated different stages in the development of reflection cracking in HMA overlays over a cracked concrete pavement as shown in **Figure 2.1**. This process can be described in two modes. In Mode 1, the progress of reflection cracking is caused by horizontal movement of concrete slabs due to the change in temperature and/or moisture. In Mode 2, the vertical load from traffic causes the differential vertical movement of cracked concrete slabs and induces a large shear stress, and hence leads to shear failure.

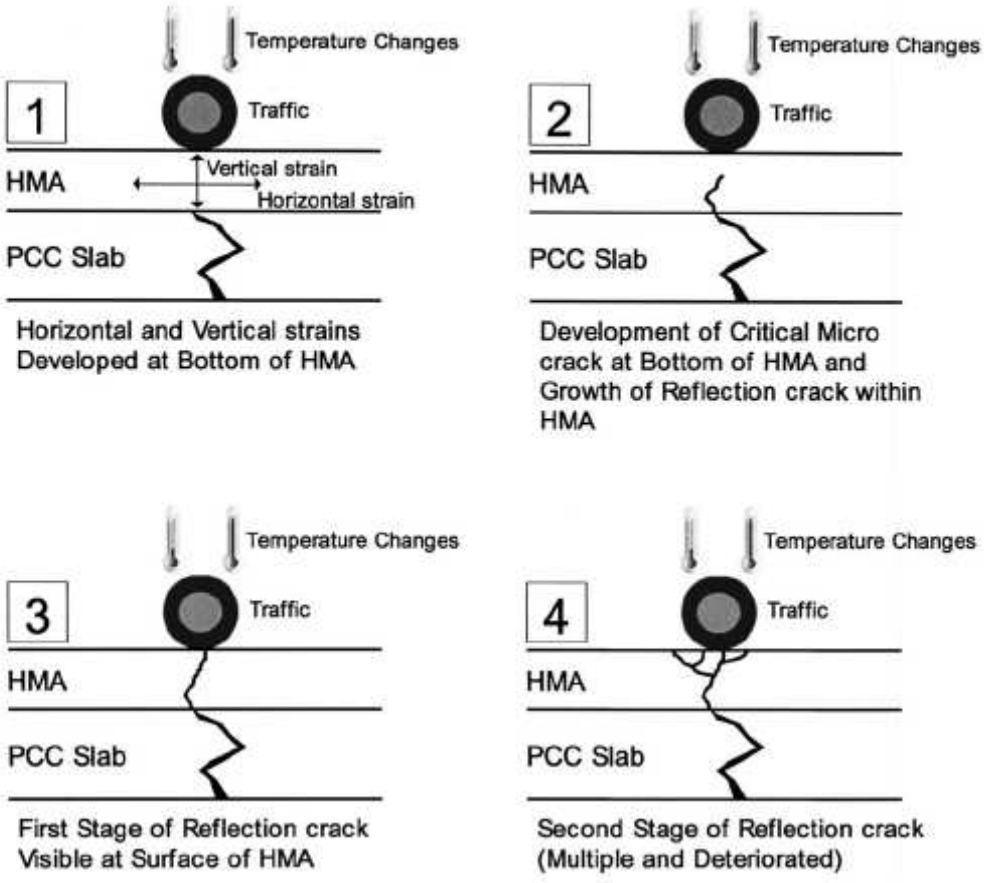

Figure 2.1 Different stages in development of reflection cracking on HMA overlays (Lee at al., 2007)

In another attempt to understand the process of reflection cracking, Francken et al. (1997) described different factors contributing to the development of reflection cracking. Traffic load can produce two types of movement in the cracked concrete slab that generate shear stresses (Figure 2.2 a and c) due to relative vertical movement of cracked slabs and flexural stresses (Figure 2.2 b) in the HMA overlay. In addition, due to temperature and/or moisture changes, the cracked concrete slab contracts and expands, inducing large tensile stress at the

bottom of HMA overlay and causing progressive opening-up of joints and cracks (Figure 2.2 d).

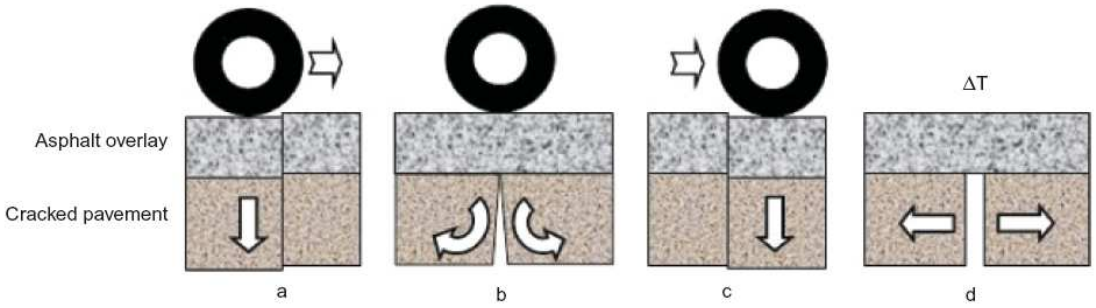

Figure 2.2 Movements in pavement joints and cracks (Francken et al., 1997)

2.3 Methods to Prevent Reflection Cracking

Literature review shows that many attempts have been made to minimize reflection cracking. These methods include installation of a transition layer made of wire mesh, steel reinforcement, and sawing and sealing at the joint, etc. Using special materials as an overlay has also been explored. Rubber asphalt, fiber-reinforced asphalt, and polymer asphalt are other commonly explored options to prevent reflection cracking. Increasing thickness of the overlay has been adopted to minimize reflection cracking. These methods have partially helped to minimize the initiation and propagation of reflection cracks (Huffman et al. 1978; NAPA 1999).

In order to delay reflection cracking, several interlayer systems have been recently introduced. These interlayer systems may delay reflective cracking by

two mechanisms: (1) reflective cracking can be retarded by using reinforcement systems, which are stiffer than surrounded materials, such as geosynthetics or steel reinforcement and (2) a low modulus material is used to create a stress absorption layer.

The methods which have been used so far can be summarized as follows:

1. Use of geosynthetic or geogrid as reinforcement. (for example, Ellis et al. 2002)
2. Use of steel as reinforcement.
3. Crack and seat treatment on the existing concrete (PCC).
4. Stress absorbing membrane as an interlayer between overlay and PCC.
5. Using modified asphalt for overlay.
6. Using large thickness of asphalt overlay.
7. Use of a porous friction course to retard reflection cracks in asphalt overlay.
8. *Rubblization* of concrete (for example, Lee et al. 2007)

Button and Lytton (2006) provided guidelines for using geosynthetics to reduce reflection cracking in HMA overlays. They addressed the following issues: (a) when to consider geosynthetic products as an option, (b) cost considerations, (c) selection and storage of geosynthetics, (d) pavement design with geosynthetics, (e) construction inspection, (f) overlay construction with geosynthetics, and (g) potential construction problems. Button and Lytton (2006) proposed three scenarios of cracking within which the use of geosynthetics would be an effective

measure. These scenarios can be categorized as: (a) when crack opening is between zero to 0.03 inch, there is no need for the use of geosynthetics as a preventive method for reflection cracking, (b) when crack opening is between 0.03 to 0.07 inch, it is effective to use geosynthetics as a preventive measure for reflection cracking, and (c) when crack opening is larger than 0.07 inch, significant movement of cracked pavements makes geosynthetics unable to withstand.

2.4. Methods to Evaluate Overlays

2.4.1. Introduction

The problem of reflection cracking in HMA overlays has been studied using different approaches including formulation of mechanistic models, numerical modeling methods, and field and laboratory experimentation. Several attempts have been made to address crack width and propagation of cracks since crack initiation and propagation is significant in understanding the process and mitigation of reflection cracking. The following sections will address laboratory studies, field studies, and theoretical approaches to investigate reflection cracking and crack initiation and propagation.

2.4.2. Laboratory Methods for Testing HMA Mix

Laboratory devices to study reflection cracking

In laboratory studies, several devices have been developed to stimulate field conditions for reflection cracking. One of the most cited tests in the study of reflection cracking is the trail developed in the Autun laboratory in France (Vanelstraete et al. 1997). The Texas overlay tester tool developed by Texas DOT in 2005 is another commonly used device in evaluating reflective cracking life of HMA overlays. Test results from the Texas overlay tester has been verified through more than five case studies in Texas and correlate well with the field performance. Lee et al. (2007) developed two set-ups in the laboratory to stimulate reflection crack mechanisms as shown in **Figure 2.3**.

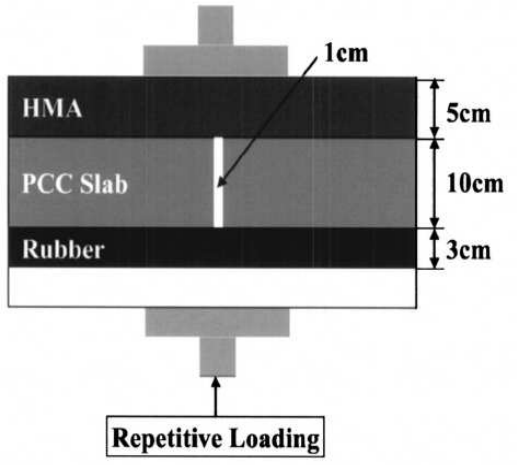

(a) Simulation of tensile strain

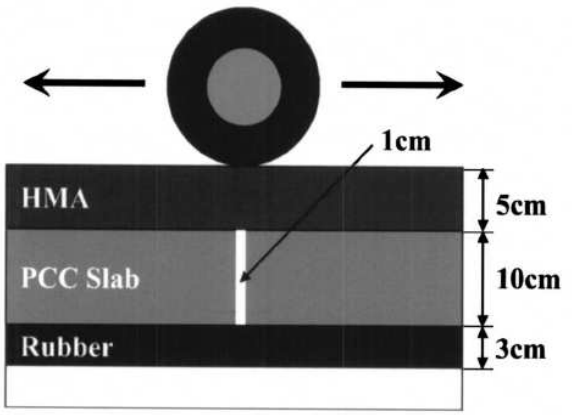

(b) Simulation of shear strain

Figure 2.3 Experimental simulation of tensile and shear strains in HMA overlays (Lee et al., 2007)

The above-mentioned laboratory devices or set-ups are intended to stimulate field conditions by creating simultaneous horizontal and vertical movements of jointed or cracked pavements thus creating tensile and shear strains at the bottom of HMA overlays.

Methods to characterize tensile strength of HMA mixture

Research has been conducted to characterize tensile strength of HMA mixture and relate it to performance of asphalt pavements. Good understanding of fracture properties of HMA is essential to limit low-temperature cracking. Low temperature cracking is one of the factors responsible for reflection cracking. A high tensile strain at failure indicates that a particular HMA can tolerate a higher strain before cracking, which means it is more likely to resist cracking than an

HMA with a low tensile strain at failure. Tensile strengths of HMA before and after water conditioning can give some indication of moisture susceptibility. If a water-conditioned HMA sample retains most of its tensile strength as compared to a dry HMA sample, this HMA can be assumed reasonably moisture resistant. The simplest and most common test method to determine fracture resistance or tensile strength of a HMA mixture is the Marshall stability test. Although the Marshall stability test is simple, it cannot properly simulate field conditions; therefore, it has been abandoned in many countries. Currently, two test methods are commonly used to measure HMA tensile strength: (a) indirect tension test and (b) thermal cracking test. Researchers have used Indirect Tensile Tests (IDT) to characterize tensile properties of HMA mixtures (for example, Huang et al. 2003).

The IDT strength test was originally developed to measure the tensile strength of Portland concrete mixtures, and was later adopted to measure the tensile strength and modulus of asphalt concrete mixtures. Christensen and his associates' study showed a good relationship between laboratory testing and field data *(*NCHRP 2003*).* In the same research, the evaluation of IDT for measuring performance of HMA at low temperature was explored. Overall tensile stress for a ruggedness study was 415 psi with a standard deviation of 50.1 psi. These two results show that temperature plays a significant role in determining the tensile strength of HMA mixes. The procedure of the indirect tension test can be found in the AASHTO TP 9 standard "Determining the Creep

Compliance and Strength of Hot Mix Asphalt (HMA) Using the Indirect Tensile Test Device".

The thermal cracking test determines the tensile strength and the temperature at fracture of an HMA sample by measuring the tensile load in a specimen which is cooled at a constant rate while being restrained from contraction. This test is terminated when the sample fails by cracking. The procedure of the thermal cracking test can be found in the AASHTO TP 10 standard "Method for Thermal Stress Restrained Specimen Tensile Strength".

Measurement of tensile strain is important for evaluating the tolerable strain the HMA can endure before initiation and propagation of cracks underneath HMA overlays and hence developing the reflection cracking. The most common method to measure the strain in an HMA specimen is attaching an extensometer at a specified location on the specimen. Recently, a more sophisticated method to measure strains in HMA specimens in laboratory has been developed which use image analysis (Masad et al. 2001). This method basically involves taking images of the HMA mix at various stage of a Georgia loaded wheel tester (GLWT) by a charged couple device (CCD) camera and analyzes them by computer resources like software MATCH. This software is used to calculate the translation and rotation of lager particles (smaller particles are considered the part of binder and eliminated manually at the image taking level) which have complex geometry. Analysis of images before and after the GLWT test gives the stain in HMA.

In recent years, the semi-circular bend (SCB) test has been used in pavement engineering to characterize the tensile behavior of HMA mixtures. SCB is a fast and accurate three-point bending test to characterize the tensile strength of HMA specimens. "SCB test is going to be an accepted method for asphalt concrete pavements" (Arabani et al 2007). SCB was adopted in our study of HMA overlays for characterizing their tensile strengths.

Methods to characterize shear strength of HMA mixtures

As reflection cracking is a result of intolerable tensile strain and shear stress in HMA overlays, measurement of shear strength of HMA mixtures is equally important as measurement of the tensile strain. Researchers have used various laboratory methods and devices to study shear strength of HMA. Probably the most common device is Superpave Shear Tester (SST).

The Superpave Shear Tester (SST) is a closed-loop system that can apply axial loads, shear loads. Pressures are applied by hydraulic mechanism to asphalt concrete specimens at controlled temperatures. The response of asphalt concrete can be used to as input data to predict performance models. Superpave Shear Test is carried out in two ways, known as the repeated shear at a constant height (RSCH) test and the fixed shear at a constant height (FSCH) test. Abd et al. (2002) introduced a test facility, which was used to assess the shear performance of HMA mixtures. They conducted the studies on four different HMA mixtures and suggested correlation between shear strength and tensile strength. Wang et al. (2005) used a triaxial device to measure shear properties

of HMA mixtures subjected to multi-stage loading. Chen et al. (2006) developed a uniaxial penetrating test to characterize the shear resistance of HMA mixtures. This test provided consistent data for selected HMA mixtures. However, these described techniques are sophisticated and unavailable to most researchers and engineers, thereby limiting the scope of determining shear resistance characteristic of HMA mixtures.

In attempt to develop a simple testing device for characterizing shear resistance of HMA mixtures, Wang et al. (2008) modified an MTS machine, which consists of two hollow cylinders of the same dimensions. HMA specimens with different diameter can be fitted between two cylinders. The two cylinders can move along a uniform plane under applied loading. Since the cylinders can move along the uniform plane, thereby inducing uniformly distributed shear stress at the middle part of the HMA specimen.

Since SST is quite expensive and requires highly trained operators to run, a simplified version of SST was developed through the National Cooperative Highway Research Program (NCHRP) project 9-7, known as Field Shear Tester (FST). Sensitivity analysis of FST showed that the value of complex modulus obtained from IDT and FST are quite similar (NCHRP 2003).

Methods to characterize fatigue behavior of HMA mixtures

Fatigue behavior of HMA mixtures is one of the most significant factors for reflection cracking. Fatigue cracking is one of three main factors (fatigue cracking, rutting, and low temperature cracking) of early failure of HMA overlays and mainly caused by repetitive traffic loading on the pavements. The cracking resistance of HMA under repetitive loading is directly related to the behavior of HMA overlays under traffic loading. Therefore, characterizing the fatigue behavior of HMA mixtures in laboratory has been focus of research for many years.

Laboratory testing methods are available to characterize the fatigue behavior of HMA mixtures. One of the most common laboratory test methods to characterize fatigue behavior of HMA mixtures is the beam fatigue test (Roberts et al., 1996). This test method is believed to possess most similar stress conditions to field HMA mixtures under repetitive traffic loading. This test is a three point loading method developed under SHRP-A-003A to evaluate the fatigue behavior of HMA mixtures. The beam fatigue test was modified in the SHRP-A-04 project to improve its simplicity and reliability.

This fatigue test uses a pneumatic beam fatigue equipment, which has a beam specimen subjected to a repeated stress or strain controlled loading. The load is applied at the center of the beam until the occurrence of failure. The test is digitally controlled and data is acquired through a software application. The

failure is defined as a 50 percent reduction in initial stiffness, which is measured from the center point of the beam after 50th load cycle. (Roberts et al. 1996)

Recently, a new way to determine the failure of a flexural fatigue test was suggested by Carpenter et al. (2003) based on the dissipated energy concept (Ghuzlen et al., 2000; Carpenter et al., 2003, and Shen et al., 2005.). In this method, the ratio of dissipated energy change is defined as a ratio of the change in the dissipated energy between two neighboring cycles divided by the dissipated energy of the first cycle.

2.4.3. Field studies to evaluate crack width and reflection cracking

As the phenomenon of reflection cracking is complex and it involves several factors acting simultaneously including traffic load, it is difficult to stimulate the exact stress condition in laboratory or using finite element models. Therefore, field studies have been carried out to closely examine the behavior of HMA overlays. The major drawback in full-scale field tests is that they are costly and time-consuming, making it hard to control test conditions over a period of time properly.

Perkin et al. (2005) constructed four full-scale flexible pavements and applied the repetitive traffic loading by a heavy simulator equipped with dual tires having a standard truck half axle. Sensors to measure stresses and strains were embedded in the pavement test sections, and a surface profiler was used to

monitor rutting. The main issue with this project was very costly and time consuming.

In the field, histogram-based machine vision was used to detect the crack ranging from 1/8 to 1 in. (3-25 mm) in width in both asphalt concrete (AC) and Portland cement concrete (PCC) pavements (Kirschke et al., 1992).

Research was conducted at IDOT according the MEPDG guidelines to compare the experimental value of crack width with theoretical one and found that for a continuous reinforced concrete pavement (CRCP), the average crack width ranged from 0.031 to 0.116mm at the steel depth at standard temperature (Erwin et al., 2005). In a similar field study, Rosleter (2007) measured the crack width varying from 0.03 to 0.1 mm and Kohler (2006) measured the crack width near the surface varying between 0.0255 and 0.0777mm for average pavement temperatures less than 10°C

.

Continuously reinforced concrete pavement (CRCP) is a concrete pavement constructed with continuous longitudinal steel reinforcement and no intermediate transverse contraction joints. During a 2-year period after construction, CRCP developed a transverse cracking pattern, with cracks typically spaced 0.6 to 1.8 m (2 to 6 ft) apart (Selezneva et al., 2007). Computer software like CRCP-10, which is based on finite element formulations, mechanistic models, and probability theories, can be used to analyze the behavior of continuously reinforced concrete pavements and to predict crack width and mean crack

spacing (Kim et al., 2003). Al-Qadi et al. (2001) suggested regression equations for flexible pavement of the strain as a function of temperature at a particular speed of vehicle based on field studies.

2.4.4. Theoretical approaches to study reflection cracking

Most of the methods to mitigate reflection cracking are developed based on laboratory results and empirical formula, which produced results from very successful to disastrous. Since the 1970s, fracture mechanics theory has been used to analyze the fatigue behavior of HMA mixtures (Majidzadeh et al., 1971). Recent researches have employed more favorable mechanistic approaches to determine fracture properties of HMA overlays using fracture mechanics theories. A fracture mechanics theory is used to understand the fundamental physical process taking place in the system. For example, a fracture mechanics theory has been used to predict fracture properties of geosynthetic interlayers and fatigue life of an asphalt pavement (Majidzadeh et al., 1976). Complex geometry and complicated stress transfer often necessitate the use of finite element methods (FEM) and computer resources to solve a large system of equations. Molenaar (1993) evaluated the reflective cracking using FEM and fracture mechanics. De Bondt et al. (1999) gave an extensive review of the phenomena of reflective cracking using FEM methods, fracture mechanics theories, as well as design procedure and the effectiveness of overlay alternatives. A new method called Calibrated Mechanistic Approach with Surface Energy (CMSE) was developed by Walubita (2006) of the University of Texas A&M, for

characterizing asphalt mixtures. This method is considered rational and promising in characterizing the asphalt mixtures (AAPT, 2006).

2.4.5 Theoretical Concepts used to address crack width in the pavement

Normally crack analysis is done either by smeared crack approach or fracture mechanics approach. The basic principle of fracture mechanics approach assumes crack as a series of inter-connected single-line segments. Propagation of crack from pre-existing defect through material takes place according to certain crack growth criteria, such as maximum energy release rate. On the other hand smeared crack approach assumes that cracks are spread over a finite region. Average tensile strain is representation of crack presence over concerned region. Material models simulatating proper compression and tension, cracking behavior of materials can be reasonably predicted by smeared crack approach (Birgisson et al., 2007). However, none of the approach can fully capture the cracks propagate randomly through weak planes. ”The explicit fracture modeling with the displacement discontinuity boundary element method has the potential to evaluate the mechanics of fracture in asphalt mixtures (Birgisson et al., 2003)”. The following figure shows the general trend of crack propagating in HMA mix based on explicit fracture modeling.

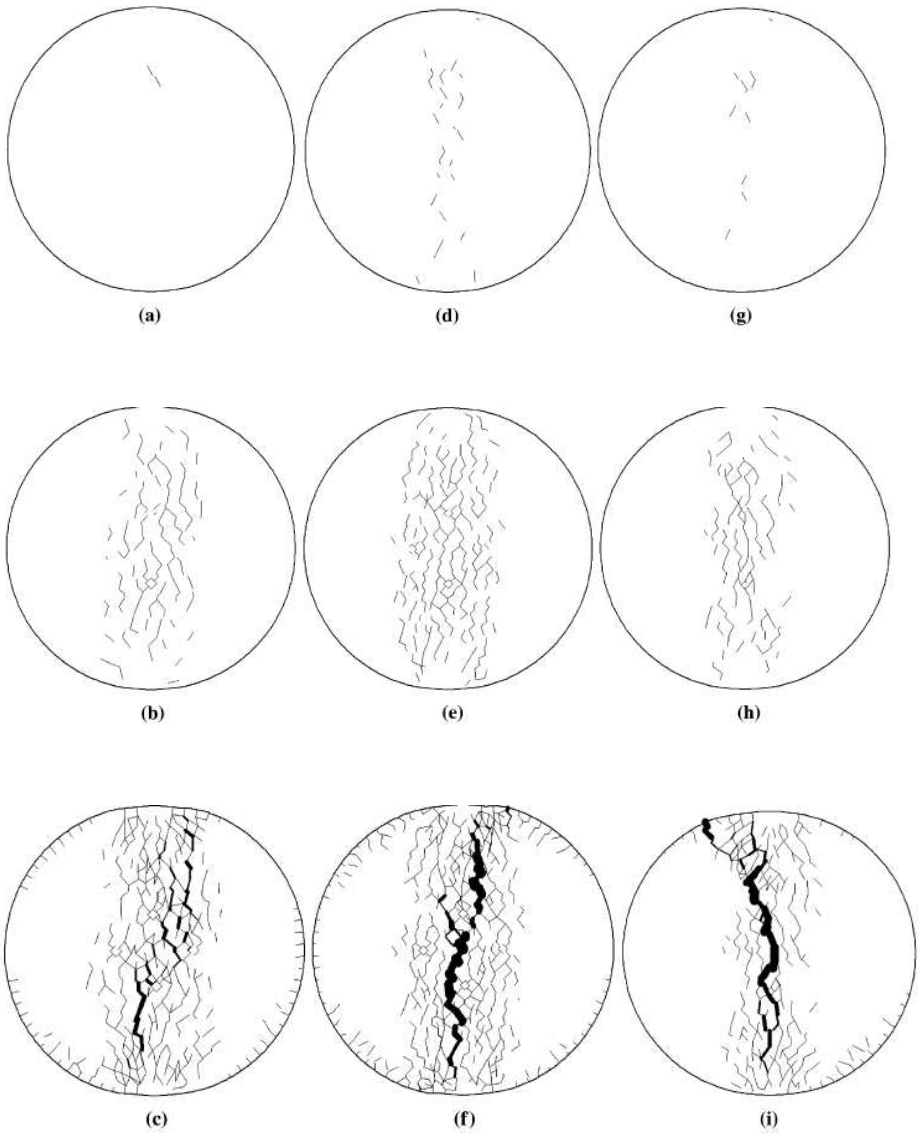

Figure 2.4. Three different mixes. (a, d, g) first crack appear, (b, e, h) crack pattern at fracture point, and (c, f, i) cracks at final load (Birginson et al., 2003)

Asphalt pavement cracking is an irreversible fracturing process caused by cyclic loading from traffic. Kumara et al. (2004) proposed a model to predict the distribution of longitudinal surface initiated wheel path crack depths based on cumulative axle load (ESAL). In-service pavements selected for study had large

sample space. A stochastic relationship was also developed between the crack width/depth ratio and cumulative ESALs based on measurements obtained from a large number of core samples.

In earlier attempt to address the propagation of crack through asphalt pavements, concepts of fracture mechanics, Paris law, and J-integral have been used (Seong et al., 2006). Castell et al. (2000) attempted to measure the crack growth experimentally. Recently, a cohesive zone model has been applied to address the fracture behavior of asphalt mix and stimulate the propagation of cracks. With the help of the cohesive concept, a model was developed and implemented with the help of the ABAQUS user-specified element. A slender double cantilever beam was chosen and analyzed. The results from this cohesive zone model remarkably matched with the analytical solution even for small cracks (Seong et al. 2006).

3 EXPERIMENTAL STUDY

This chapter comprises of four sections: (1) test equipment used in the study, (2) material characterization, (3) Sample preparation, and (4) test procedure.

3.1 Test Equipment

This section describes different test apparatus that were used in this study.

3.1.1. Superpave gyratory compactor

The Superpave gyratory compactor is a transportable device. It is used to fabricate HMA specimens by simulating construction and traffic on an asphalt pavement. The specimens fabricated with the gyratory compactor can be used to determine the volumetric properties (air voids, voids in the mineral aggregate, and voids filled with asphalt) of Superpave mixes. These properties, measured in the laboratory, indicate how well the mix meets design criteria. Thus gyratory compactor can be used for quality control/quality assurance. This equipment can also be set up at a job site to verify that the delivered asphalt mix meets the job mix volumetric specifications.

The superpave gyratory compactor prepares specimens that represent actual in-service pavements in terms of compaction and traffic loads. The level or amount

of compaction is dependent on environmental conditions and traffic levels expected at a job site.

To create a mix with a high degree of internal friction and high shear strength, the Superpave mix design procedures include requirements for aggregate angularity and gradation. The design goal is the production of a strong stone skeleton which resists rutting, yet includes enough asphalt and voids to improve the durability of the mix.

Sample height, number of gyrations as well as pressure to be applied can be set in the Superpave gyratory compactor as shown in **Figure 3-1**.

Figure 3.1. Pine Superpave Gyratory Compactor Control Panel

3.1.2 Direct shear box

Direct shear box is generally used to determine shear resistance of soil. The box comprises of two rectangular sections placed on each other. A screw system can be used to adjust the spacing between two sections. When the top section is fixed with help of clamps, the lower section moves at a specified speed causing the shearing of the specimen prepared. Once the horizontal displacement of the lower moving section reaches a specified value, the test stops automatically. The common issue in using direct shear box to characterize shear resistance of soil is non-uniform distribution of shear stresses along the shearing surface (Brown et al 2000). It is known that stresses at the corner are much more than the central part (DeBondt 1999). Since the HMA samples used in this study are 1.5 and 2.0 in. thick, the non-uniformity of shear stresses across the samples should not be an important issue. **Figure 3.2** shows cross-sectional view of the direct shear box test.

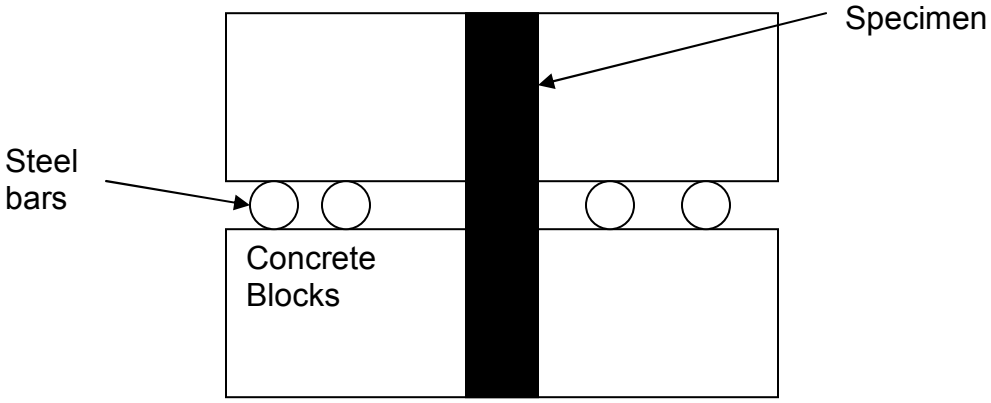

Figure 3.2 Cross-sectional view of direct shear box set-up

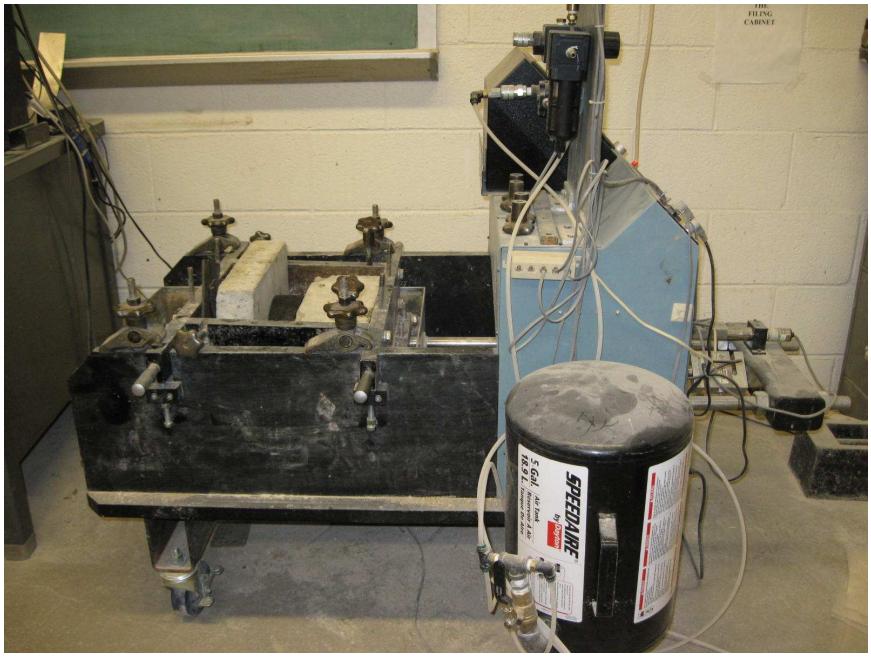

Figure 3.3 Direct shear box test used in study.

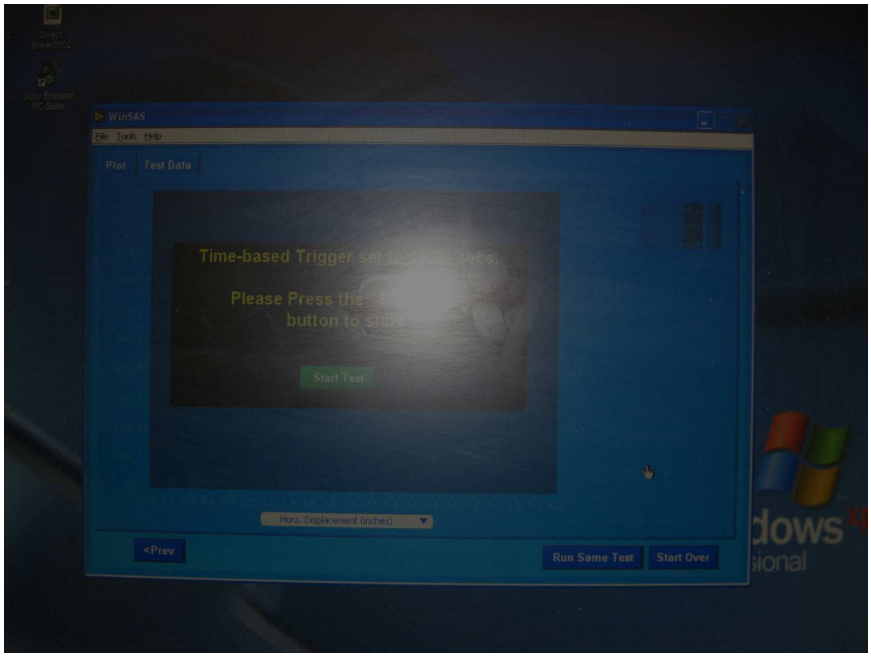

Figure 3.4. Control panel for data acquisition from direct shear box test

3.1.3. Semi-circular bend setup

The principle and basic setup of a semi-circular bend test to determine the tensile strength of an HMA sample is shown in Figure 3.4. The actual equipment used in this study is shown in Figure 3.5. Monotonic and cyclic loading can be applied to the semi-circular HMA specimen until failure. The loading rate for the monotonic loading on HMA samples is generally 2 in/min. The center to center distance between two rollers is 80% of the sample diameter. The semi-circular bend test was previously used in rock mechanics to study the crack propagation and to determine tensile strength of rock. In recent years, several studies have been conducted to evaluate the tensile behavior of HMA mixes, for example, Krans et al. (1996), Molenaar et al. (2002), and Huang et al. (2004).

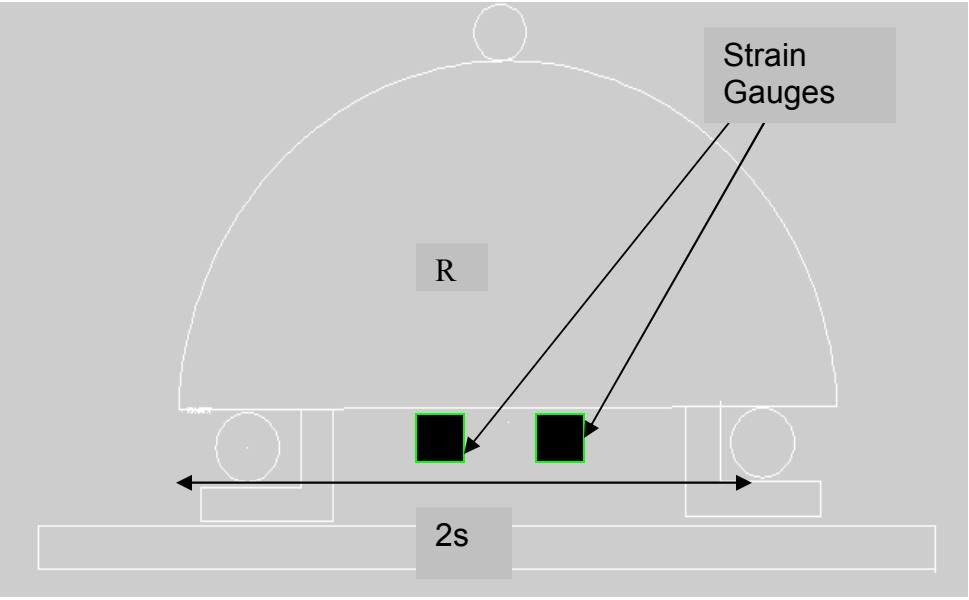

Figure 3.5. Systematic diagram for semi-circular bend test

In Figure 3.4, r is the radius of the semi circular specimen, 2s is the center to center distance between support rollers. The diameter of the horizontal loading strip is 9.4mm while the diameter of the two supporting strips is 6.25mm.

The maximum tensile stress at the bottom of the specimen can be calculated from the following equation, which was obtained from a finite element analysis (Molennar et al. 2002 and Huang et al. 2004):

$$\sigma_x = 3.564 \frac{P_{ult}}{Dt}$$

where

σ_x = maximum tensile stress (MPa)

P_{ult} = peak load (N)

t = thickness of the specimen (mm)

D = diameter of the specimen (mm)

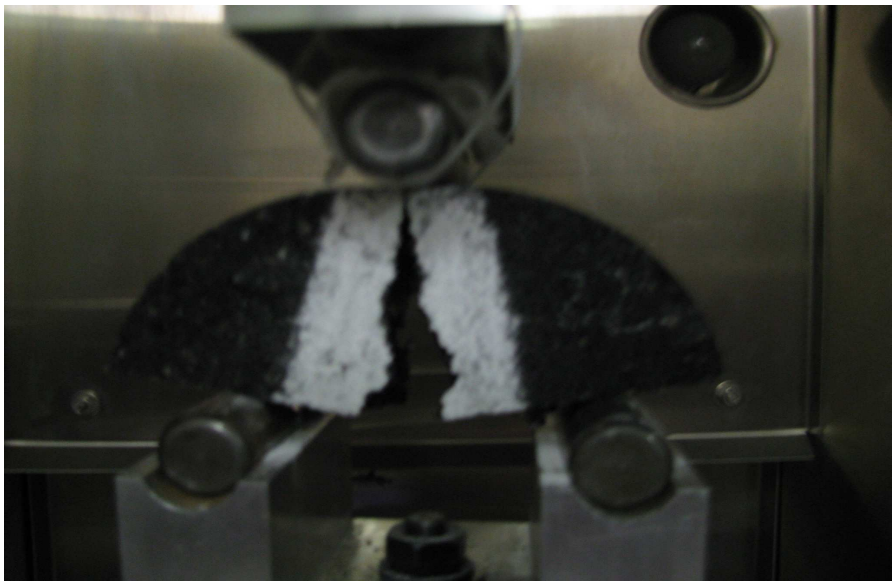

Figure 3.6. Semi-circular bend set up.

3.2 Material Characterization:

Materials from two KDOT's projects, namely 089 C-4318-01 (Mix 1) and 56-29 KA-1087-01 (Mix 2), were selected for this study. Mix design SM 12.5 A was used for both mixes. Direct shear box and semi-circular bend tests were conducted on both mixes.

3.2.1 Asphalt binder

Bitumen used for HMA specimens was from Hamm Contractor. Two types of binder, PG 64-22, and PG 76-22, were chosen for this study, in which PG 64-22 binder was used for Mix 1 and PG 76-22 was used for Mix 2. The specific gravity values of these two asphalt binders were 1.0410 and 1.0400, respectively. The recommended asphalt content for Mix 1 was 6.25 percent and that for Mix 2 was 5.6 percent.

3.2.2 Aggregate and mix design specification

HMA Mix 1

The percentage of aggregates used in HMA Mix 1 and their specific gravity values are presented in Table 3.1. The sieve analysis for aggregates used in HMA Mix 1 is presented in Table 3.2. The mix design specification for Mix 1 is

presented in Table 3.3. Figure 3.7 and 3.8 show the gradations of aggregates used make test specimens for mix 1 and mix 2.

Table 3.1 Percentage of aggregates used in HMA Mix 1 and their Specific Gravity values

Aggregate designation	Percentage in Mix	Specific Gravity
CS-1	12	2.518
CS-1A	34	2.521
MSD	43	2.538
SSG	11	2.599
Binder PG 64-22	Total= 100	Combined Aggr. Sp. Gr. 2.536

Table 3.2 Sieve analysis for aggregates used in HMA Mix 1

Sieve # (% passing)	CS-1	CS-1A	MSD	SSG
1	0	0	0	0
3/4	0	0	0	0
1/2	64	0	0	0
3/8	95	13	0	0
4	97	81	0	0
8	98	97	30	11
16	98	97	60	32
30	98	97	81	62
50	98	97	91	90
100	98	97	94	98
200	98	97	95	99.5

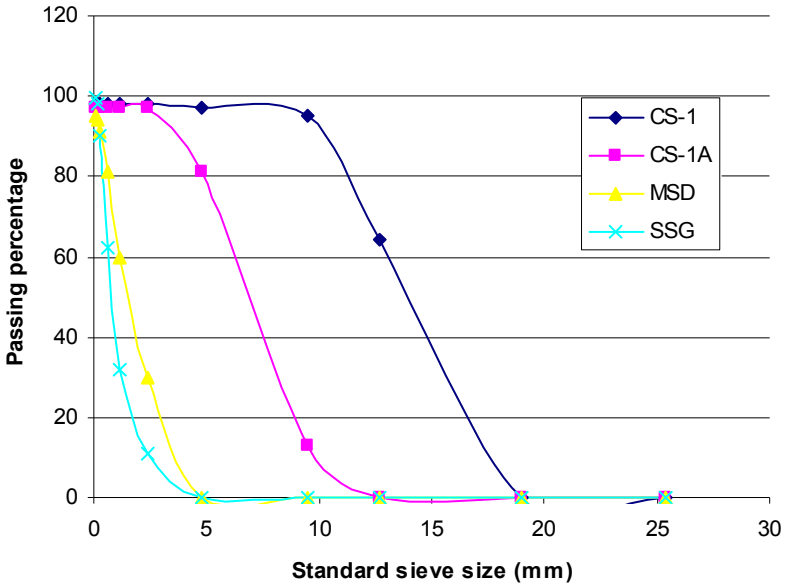

Figure 3.7 Aggregate gradations used for test specimens, mix 1.

Table 3.3 Mix design specification for Mix 1

% AC by mass mix	6.250
% Aggr. By mass of mix	93.750
Sp. Gravity of AC	1.0410
Bulk Sp. Gr. of aggregate	2.536
Max Sp. Gr.	2.410
Bulk Sp. Gr. of mix	2.310
Effective Sp. Gr. of aggregate	2.641
Absorbed %AC	1.632
Effective AC	4.720
%VMA	14.6
% Air Voids	4.15
% VFA	72
Effective film thickness	10.73
Dust/binder ratio	1.1

Table 3.4 Guidelines for preparation of specimens for HMA Mix 1

Mix design	SM 12.5A
Mixing temperature range (F)	302-313
Molding temperature range	282-291
Nini Gyrations	7
Ndsg Gyrations	75
Nmax Gyrations	115
% Asphalt Content	6.25

Specification for aggregate for Mix 2

The percentage of aggregates used in HMA Mix 2 and their specific gravity values are presented in Table 3.5. The sieve analysis for aggregates used in HMA Mix 2 is presented in Table 3.6. The mix design specification for Mix 2 is presented in Table 3.7.

Table 3.5 Percentage of aggregates used in HMA Mix 2 and their specific gravity values

Aggregate designation	Percentage in Mix	Specific Gravity
CG-1	20	2.578
CG-2	25	2.581
CG-3	25	2.581
SSG-2	30	2.594
Binder PG 76-22	Total= 100	Combined Aggr. Sp. Gr. 2.584

Table 3.6 Sieve analysis for aggregate used in HMA Mix 2

Sieve # (% passing)	CG-1	CG-2	CG-3	SSG-2
1	0	-	-	0
3/4	0	-	-	0
1/2	36	0	0	2
3/8	70	0	0	4
4	96	10	11	13
8	97	40	43	41
16	98	57	62	70
30	98	67	74	85
50	98	76	83	95
100	98	84	91	99
200	98.2	91	95	99.2

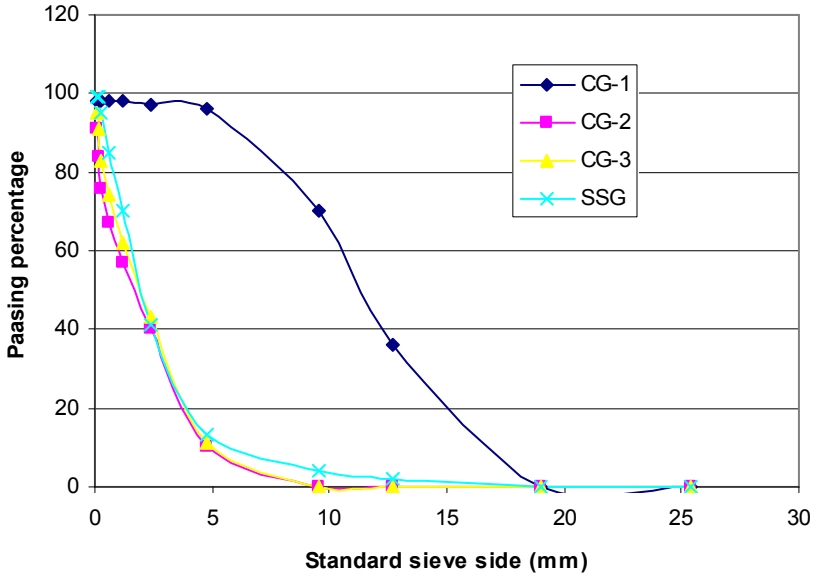

Figure 3.8 Aggregate gradations used for test specimens, mix 2.

Table 3.7 Mix design specification for Mix 2

% AC by mass mix	5.50
% Aggr. By mass of mix	94.500
Sp. Gravity of AC	1.0400
Bulk Sp. Gr. of aggregate	2.584
Max Sp. Gr.	2.408
Bulk Sp. Gr. of mix	2.292
Effective Sp. Gr. of aggregate	2.613
Absorbed %AC	0.447
Effective AC	5.078
%VMA	16.2
% Air Voids	4.82
% VFA	69
Effective film thickness	10.32
Dust/binder ratio	0.7

Table 3.8 Guidelines for preparation of specimens for HMA Mix 2

Mix design	SM 12.5A
Mixing temperature range (F)	310-340
Molding temperature range	295-320
Nini Gyrations	8
Ndsg Gyrations	100
Nmax Gyrations	160
Design Asphalt Content %	5.6

3.3. Sample Preparation

Cylindrical samples were prepared for direct shear and semi-circular bend (SCB) tests. Diameter of all the samples was 150 mm. Samples can be categorized in two sets based on their thickness (a) samples having thickness 2 in and (b) samples having thickness 1.5 in. All samples are prepared at KU using the Superpave gyratory compactor. Two types of mixes (Mix 1 and Mix 2) were used for this study. The contents of asphalt binder used in this study were 6.25 percent for Mix 1 and 5.6 percent for Mix 2, respectively.

Mix and compaction temperatures were selected based on the requirements of KDOT design as shown in Tables 3.4 and 3.8. Aggregates were weighed and heated in oven to the desired mix temperature as shown in **Figure 3.9** and then mixed with binder in a mechanical mixer as shown in **Figures 3.10 to 3.11**. A hand scoop was also used to mix and to make sure aggregates were mixed properly. The mix was then heated for two hours for short term aging as shown in **Figure 3.12**.

The Pine Superpave gyratory compactor was used to compact the samples. Gyratory molds, the mix pouring funnel, the scoop were all heated to the compaction temperature. After two hours of short term aging, the required quantity of HMA mix for one sample was poured in the gyratory mold using the sample pouring funnel as shown in **Figure 3.13**. The mold was then placed inside the gyratory compactor chamber as shown in **Figures 3.14 to 3.15** and

the door was closed. The number of gyrations, the sample height, and the required compaction pressure were set on the control panel. In this study, the compaction pressure was set at 600 kPa and the number of gyrations was set at 75 and 100 for Mix 1 and Mix 2, respectively. The base of the compactor inclined to 1.25^0 and the load was applied from upper and lower plates. The compactor stopped itself when either the set height or the number of gyrations was reached. Once the machine self parked, the door was opened and the compacted sample was removed from the chamber and extruded using the hydraulic jack on the side of the compactor as shown in **Figure 3.17.**

Figure 3.9 Heating of materials and binder to reach desired temperature

Figure 3.10 Mixing of heated materials in the mechanical mixer

Figure 3.11 Pouring of a mix into a pan

Figure 3.12 Short-term aging of a mix

Figure 3.13 Heating of the gyratory compaction mold

Figure 3.14 Pouring of the mix into a heated mold

Figure 3.15 Placing of a mold into the Superpave gyratory compactor

Figure 3.16 Mold inside the Superpave gyratory compactor

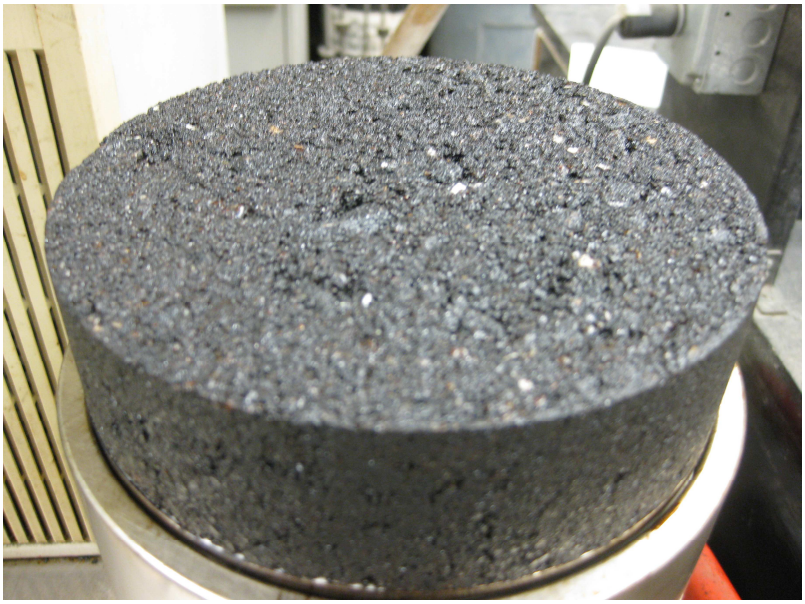

Figure 3.17 Extruding of a sample out of the mold

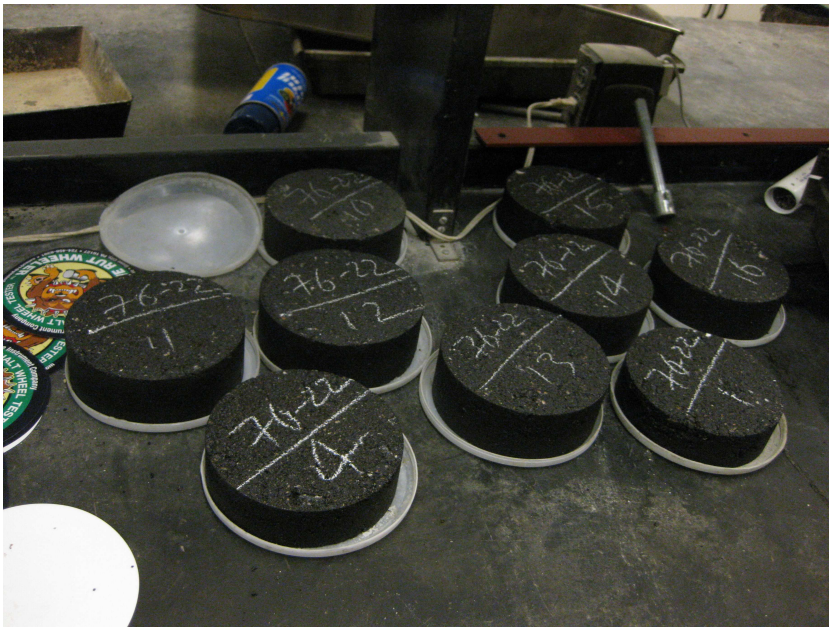

Figure 3.18 Prepared samples

3.4 Test Procedure

This section describes the test procedures for the direct shear box and the semi-circular bend test.

3.4.1 Direct shear box

A circular sample prepared by the Superpave gyratory compactor was placed into the direct shear box. With the help of concrete blocks, bending of the HMA specimen was restricted. Steel bars (**Figure 3.19**) were placed between the upper and lower portions of concrete blocks to create spacing which simulates the crack width in underlying cracked concrete slabs. **Figures 3.20 to 3.23** show

the systematic steps of setting up the specimen. Once the specimen was set up, a shearing speed was set at 0.1 in/min and a maximum horizontal displacement was set to be 1 in, with the help of the control panel. Data acquisition was done by the WINSAX program. Once all the required parameters were set up, the WINSAX application was opened in the computer. This application required various parameters to be checked and details about the specimen to be added. Once all the parameters were set in the application, a consol window appeared asking for the start of the test. Both the direct shear box and the RUN button in the consol were pressed at same time. The test started and data started to be recorded after 10 sec. The test ran until the horizontal displacement of the lower section of the direct shear box reached 0.5 in. After that the test stopped and a file was saved in the folder on the computer. All the tests were conducted at room temperature, $25 \pm 1^0 C$. **Figure 3.24** shows the appearance of the sample after failure.

Figure 3.19. Steel bar used to simulate the crack width

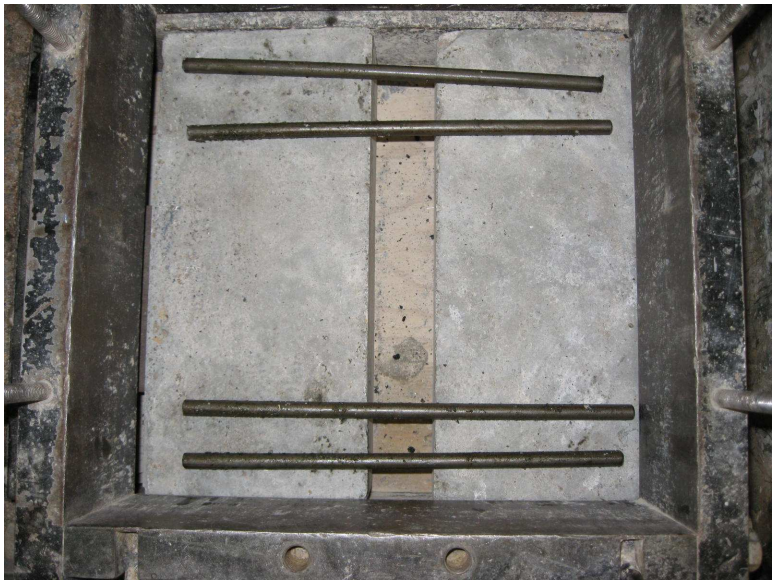

Figure 3.20. Steel bars placed over concrete blocks

Figure 3.21 An HMA sample placed between two concrete blocks

Figure 3.22 Two concrete blocks placed on the top of steel bars

Figure 3.23 The HMA sample between lower and upper concrete blocks

Figure 3.24 The failed sample after the direct shear box test

3.4.2 Semi-circular bend test

All the semi-circular bend tests were conducted at the transportation material lab at the University of Tennessee. Both static and cyclic fatigue tests were conducted on the two HMA mixes. The test procedure is described below for both cases. The entire tests are conducted at temperature $20 \pm 1^0 C$. **Figure 3.25** shows the setup for a semi-circular bend test while **Figure 3.26** shows the appearance of the failed. A white patch was made in the middle of the sample surface with chalk to assist better visual aid in recognizing the first crack appearance during the cyclic test.

Figure 3.25. A semi-circular bend test with a strain gauge attached to the bottom of the specimen

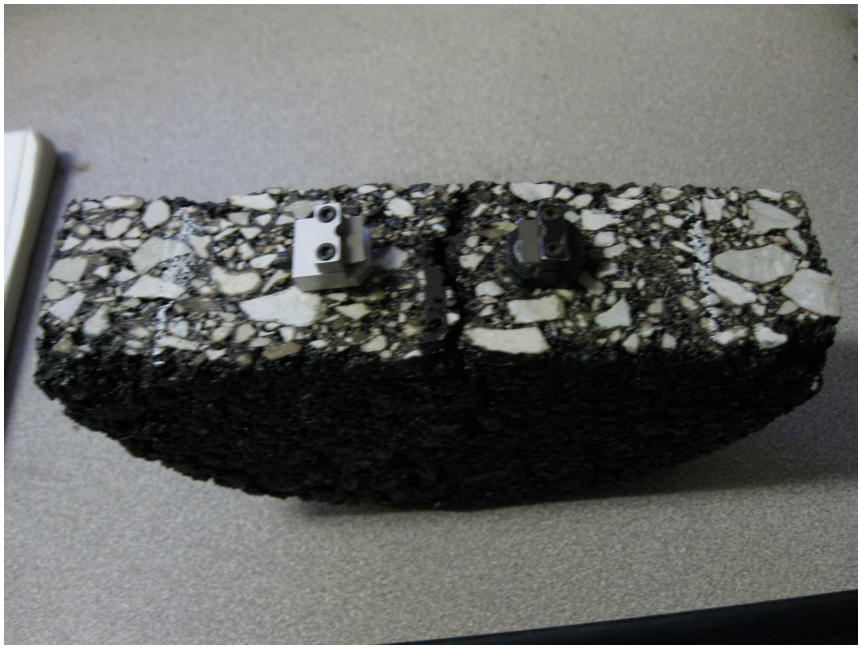

Figure 3.26. Appearance of a failed sample after testing

Procedure for a static SCB test

Step 1: Set the loading rate in the MTS machine at 2in/ min.

Step 2: Attach the extensometer to the sample at bottom of the specimen.

Step 3: Place the semi-circular HMA test sample to the holding frame (specifically made for SCB tests) attached to the MTS machine.

Step 4: Check all the connections and launch the software to control the loading and record the test data.

Step 5: Start loading the sample.

Step 6: When sample fails, stop the test.

Procedure for a cyclic fatigue SCB test

Step 1: Set the loading pattern in the MTS machine having a frequency of 1.0 Hz. The loading pattern follows 0.05 sec. loading, 0.05 sec. unloading, and rest for 0.9 sec.

Step 2: Set the load at a fraction (80%, 70%, 60%, 50%, 40% and 30%) of the maximum load from the static load tests.

Step 3: Attach the extensometer to the sample at the bottom of specimen.

Step 4: Place the semi-circular HMA test sample to the frame attached to MTS machine

Step 5: Check all the connections and launch the software to control the loading and record the test data.

Step 6: Start loading the sample.

Step 7: Once the extensometer reaches the limit (from which it will not record any data) before the sample fails (visual inspection), stop the MTS machine and adjust the extensometer so that more data can be recorded) and re-start the test.

Step 8: When the sample fail, stop the test.

4. TEST RESULTS AND DISCUSSION

This chapter comprises of two sections dealing with (a) test results obtained from direct shear box tests and static and cyclic semi-circular bend tests and (b) analysis and discussion of test results.

4.1 Test Results

Test results from direct shear box and semi-circular bend tests are presented in this section.

4.1.1 Direct shear tests

Direct shear tests were conducted on HMA Mix 1 and Mix 2 samples with thickness of 1.5 and 2 in. To simulate crack width in field, three different gaps (0.25, 0.375, and 0.5 in.) between concrete blocks were used by steel rods of different diameters. **Figures 4.1 and 4.2** show the typical load-displacement curves for Mix 1 and Mix 2 samples. It is shown that the shear load increased with the horizontal displacement and reached the peak load before decreased. The measured peak shear loads for Mix 1 samples with thickness of 1.5 and 2.0 in. are tabulated in **Tables 4.1-4.4**.

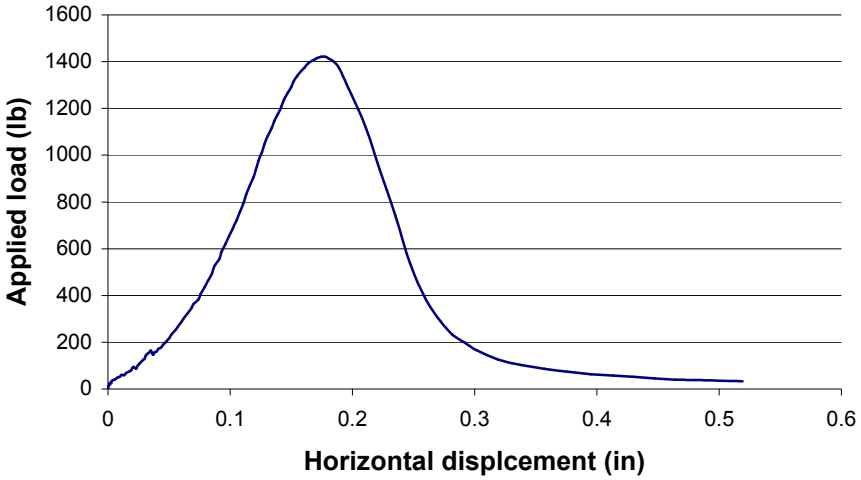

Figure 4.1. Load-displacement curve for 2 in. thick Mix 1 sample (PG64-22 binder, crack width of 0.25 in., and bulk specific gravity of 2.223)

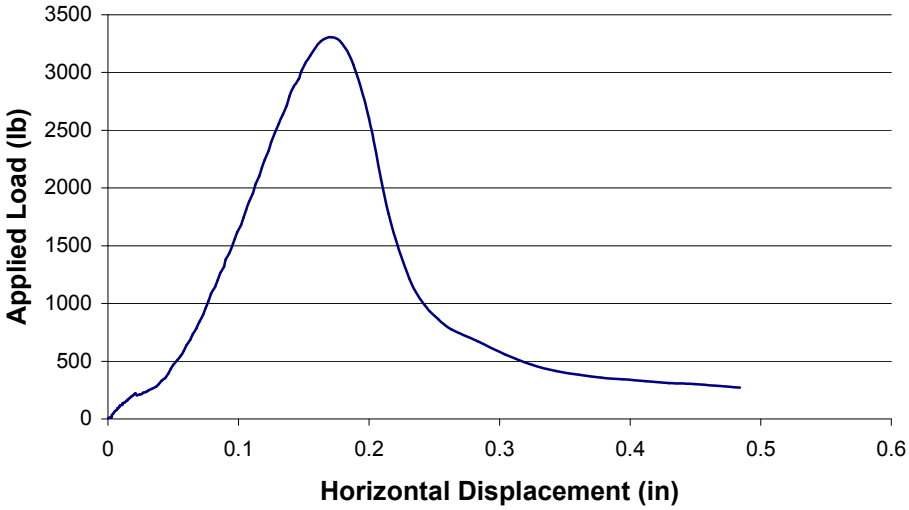

Figure 4.2 Load-displacement curve for 2 in. thick Mix 2 sample (PG 76-22 binder, crack width of 0.25in, and bulk specific gravity of 2.340)

Table 4.1. Peak shear loads by direct shear tests for 1.5 in. thick Mix 1 samples

Sample #	Simulated Gap (in)	Bulk Sp. Gr.	Peak Load (lb)
1	0.5	2.214	1117
2	0.5	2.199	897
3	0.5	2.199	1092
4	0.375	2.221	1194
5	0.375	2.230	1161
6	0.375	2.251	1353
7	0.25	2.143	852
8	0.25	2.191	928
9	0.25	2.180	989

Table 4.2. Peak shear loads by direct shear tests for 2 in. thick Mix 1 samples

Sample #	Simulated Gap(in)	Bulk Sp. Gr.	Peak Load (lb)
1	0.5	2.285	1829
2	0.5	2.265	1825
3	0.5	2.230	1385
4	0.375	2.245	1774
5	0.375	2.244	1366
6	0.375	2.257	1536
7	0.25	2.196	1100
8	0.25	2.191	1633
9	0.25	2.223	1421

Table 4.3. Peak shear loads by direct shear tests for 1.5 in. thick Mix 2 samples

Sample #	Simulated Gap (in)	Bulk Sp. Gr.	Peak Load (lb)
1	0.5	2.263	2511
2	0.5	2.306	2333
3	0.5	2.294	2412
4	0.375	2.310	2305
5	0.375	2.303	2484
6	0.375	2.301	2368
7	0.25	2.291	2816
8	0.25	2.264	2131
9	0.25	2.278	2696

Table 4.4. Peak shear loads by direct shear tests for 2 in. thick Mix 2 samples

Sample #	Simulated Gap (in)	Bulk Sp. Gr.	Peak Load (lb)
1	0.5	2.377	3073
2	0.5	2.365	3385
3	0.5	2.356	3347
4	0.375	2.370	3083
5	0.375	2.366	2968
6	0.375	2.316	2685
7	0.25	2.323	2801
8	0.25	2.340	3135
9	0.25	2.340	3307

4.1.2 Semi-circular bend tests

Semi-circular bending tests were conducted on samples of both mixes at thickness of 1.5 in. and 2 in. under static and cyclic fatigue loading. A constant loading rate at 2 in./min was applied for the static load tests. A sinusoidal loading (0.05sec loading, 0.05 unloading, and 0.9 sec rest period) of frequency 1Hz was applied for the cyclic fatigue tests. Amplitude of sinusoidal loading was a fraction of the peak compressive load obtained from the static tests. Strain was measured with a help of a strain gauge attached to each specimen. All the data acquisition was done with the help of MTS software. Nature of cyclic loading is shown in **figure 4.3**.

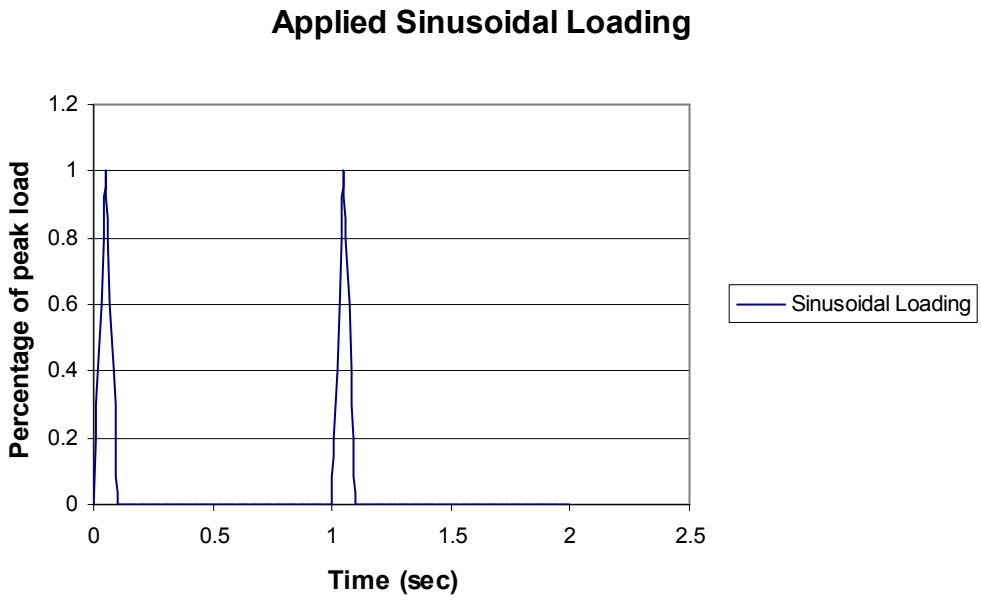

Figure 4.3 Loading pattern used for cyclic SCB tests

For each static loading test, the maximum or peak compressive load a specimen could take and the strain induced at the bottom of the HMA semi-circular sample were recorded. **Figures 4.4** and **4.5** show typical compressive load vs. strain curves from static loading tests on two samples at thickness of 2 and 1.5 in. The static test results for Mix 1 and Mix 2 samples are tabulated in **Tables 4.5 and 4.6**.

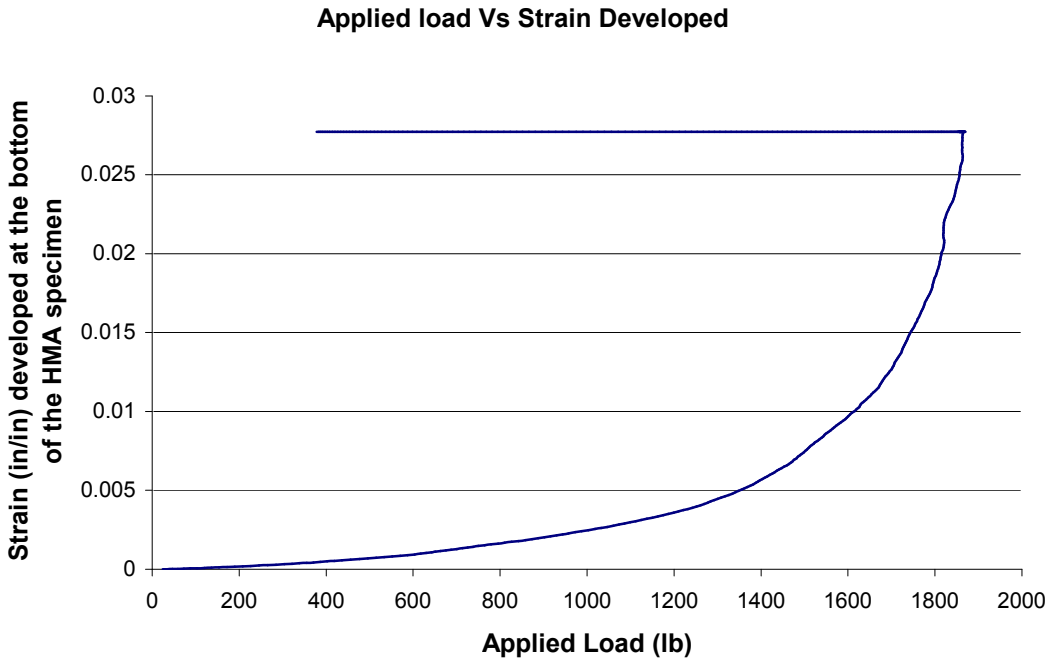

Figure 4.4. The applied compressive load vs. the strain developed at the bottom of 2 in. thick Mix 1 sample

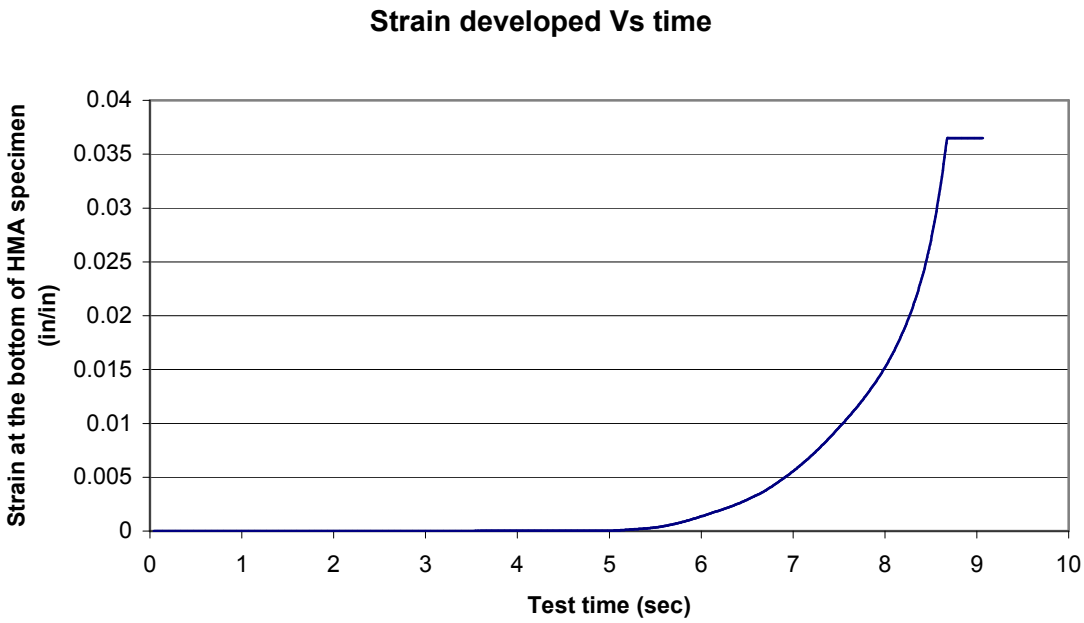

Figure 4.5. The applied compressive load vs. the strain developed at the bottom of 1.5 in. thick Mix 2 sample

Table 4.5. Static test results for Mix 1

Sample #	Thickness (in)	Bulk Specific Gravity	Peak Load (lb)
1	1.5	2.214	1650.08
2	1.5	2.220	1444.75
3	2.0	2.197	1868.72
4	2.0	2.218	2276.21

Table 4.6. Static test results for Mix 2

Sample #	Thickness (in)	Bulk Specific Gravity	Peak Load (lb)
1	1.5	2.300	2244
2	1.5	2.287	2494
3	1.5	2.287	2610
4	2.0	2.354	4174
5	2.0	2.360	3932
6	2.0	2.370	4328

Cyclic SCB tests were conducted at a fraction of the peak compressive load obtained from the static tests for Mix 1 and Mix 2. The pattern of one load cycle is shown in **Figure 4.3** while the typical pattern of load cyclic is shown in **Figure 4.6**. The strains at the bottom of each sample with time were measured continuously. **Figure 4.7** shows a typical example of the strain vs. test time curve. **Tables 4.7 and 4.8** summarize the test results from cyclic SCB tests for Mix 1 and Mix 2, respectively.

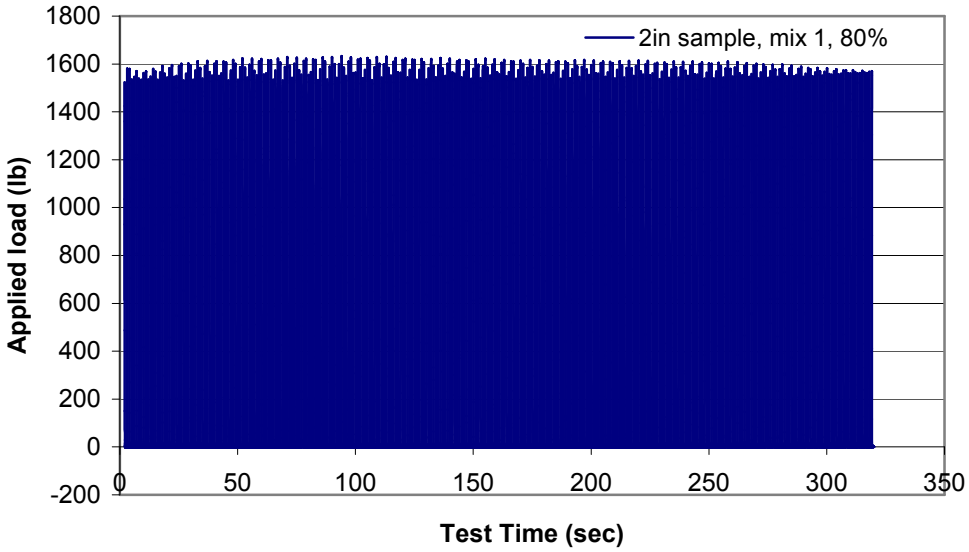

Figure 4.6. Cyclic loading for an SCB test of a 2 in. thick Mix 1 sample

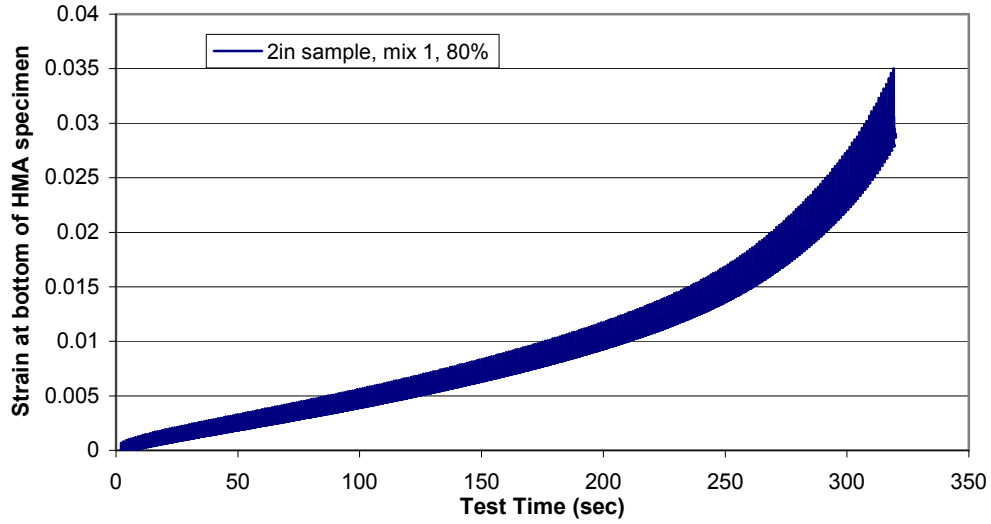

Figure 4.7. Strains developed at the bottom of the specimen vs. the test time for a 2 in Mix 1 sample

Table 4.7. Static test results of SCB tests for Mix 1

Sp. Gr.	Thickness (in)	Fraction (%)	Load (lb)	First crack (sec)	Test time(sec)
2.212	1.5	80	1200	34	74
2.241	1.5	70	1050	220	412
2.221	1.5	60	900	37	72
2.245	1.5	50	750	224	415
2.213	1.5	40	600	818	1298
2.232	1.5	30	450	820	1822
2.217	2.0	80	1600	296	341
2.229	2.0	70	1400	330	374
2.231	2.0	50	1000	1258	1637
2.246	2.0	50	1000	1133	1411
2.236	2.0	30	600	11170	13475

Table 4.8. Static test results of SCB tests for Mix 2

Sp. Gr.	Thickness (in)	Fraction (%)	Load (lb)	First crack (sec)	Test time(sec)
2.304	1.5	80	1960	10	18
2.296	1.5	70	1715	175	173
2.277	1.5	60	1470	695	431
2.322	1.5	50	1225	355	369
2.289	1.5	50	1225	170	182
2.293	1.5	40	980	968	1216
2.274	1.5	30	735	3848	4951
2.392	2.0	80	3315.2	63	65
2.378	2.0	70	2900.8	140	169
2.377	2.0	60	2486.4	150	180
2.375	2.0	50	2072	645	691
2.333	2.0	40	1657.6	673	733
2.393	2.0	30	1243.2	6274	6827

4.2 Discussions

4.2.1 Direct shear box test

Load-displacement curves obtained from direct shear box tests were used to determine the shear displacements of the HMA specimens at the peak loads. Prior to such determination, each load-displacement curve was corrected for the initial part of the curve. Because of seating errors between an HMA sample and concrete blocks, the initial portion of the load-displacement curve does not give an accurate response of the HMA specimen as shown in **Figure 4.8 a**. To correct this error, the whole load-displacement curve should be shifted towards the origin by a certain amount of offset. The required offset was determined by drawing a straight line on the linear portion of the load-displacement curve to intercept the horizontal displacement axis. **Figures 4.8 b and c** shows the detailed steps to correct a typical load-displacement curve obtained from a direct shear box test. Once the load-displacement curve was corrected, the shear displacement at the peak load was determined. **Tables 4.9 to 4.12** show the shear displacements at their corresponding peak loads for all the HMA specimens tested.

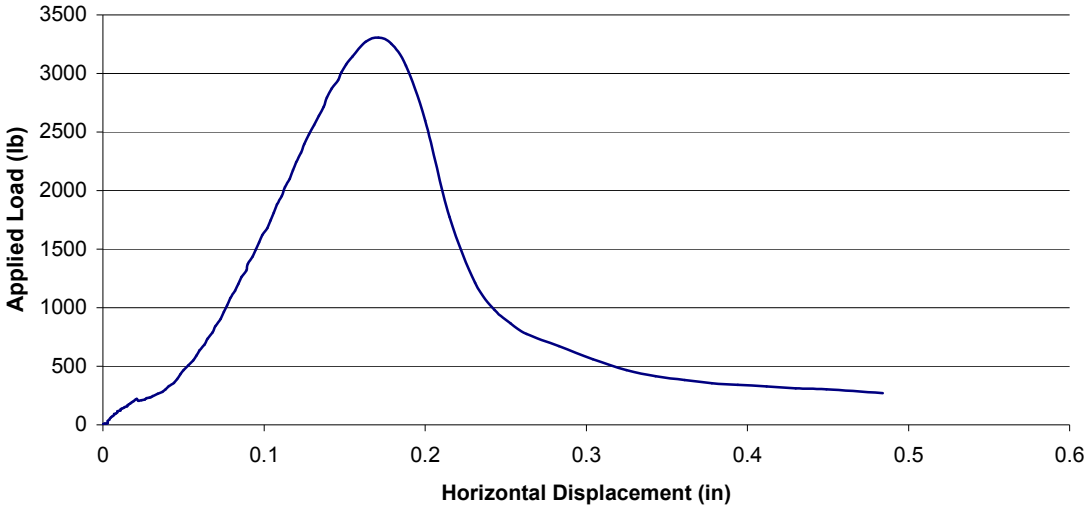

Figure 4.8 a. An uncorrected load-displacement curve obtained from the direct shear box test

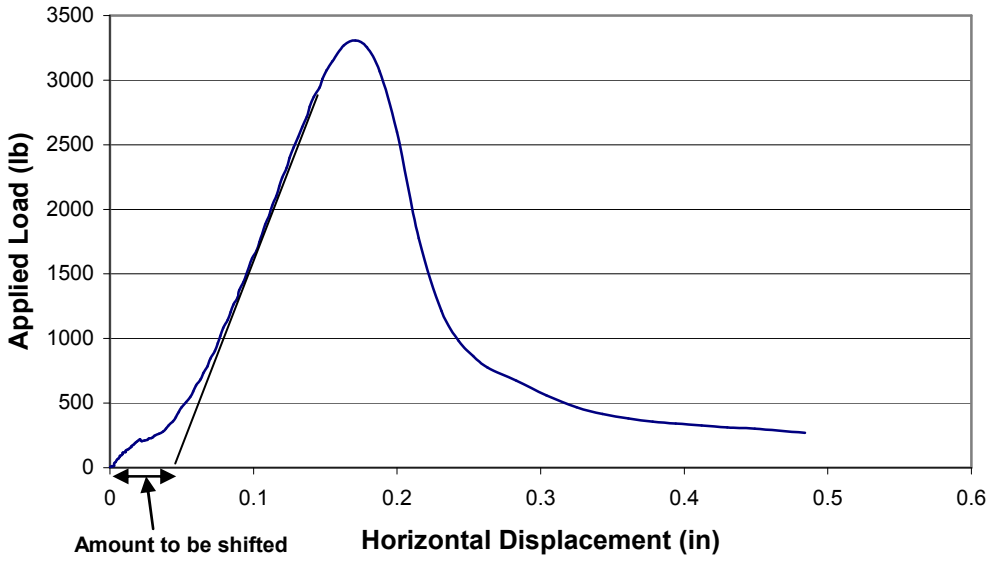

Figure 4.8b. Determination of the required offset for the load-displacement curve

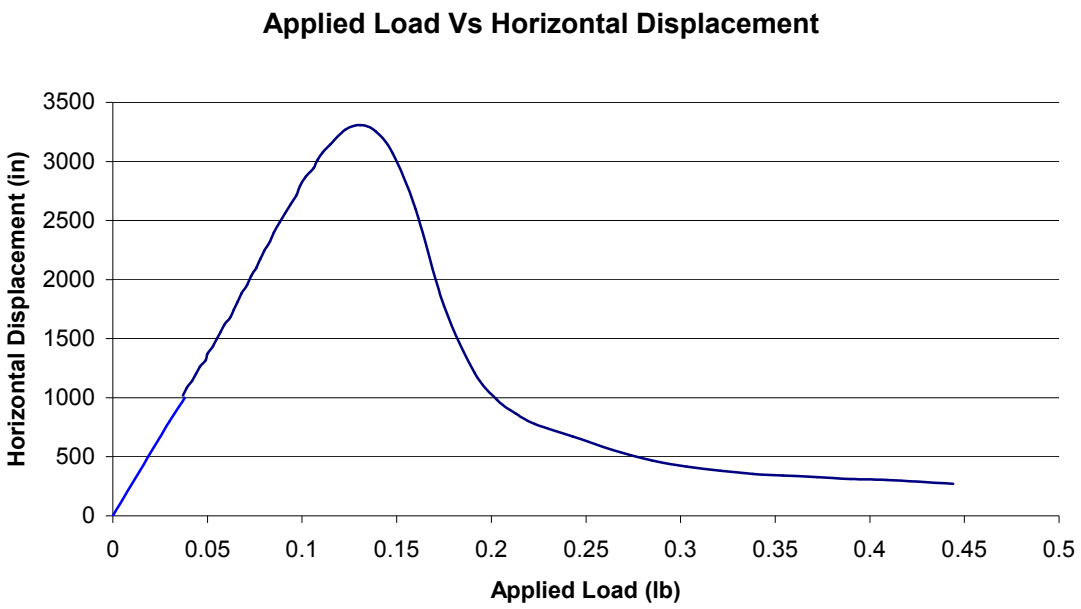

Figure 4.8c. Corrected load-displacement curve

Table 4.9 Displacements at the peak loads for 1.5 in. Mix 1 samples

Simulated Gap (in)	Bulk Sp. Gr.	Peak Load (lb)	Shear Displacement (in.)
0.5	2.214	1117	0.110
0.5	2.199	897	0.131
0.5	2.199	1092	0.141
0.375	2.221	1194	0.133
0.375	2.230	1161	0.119
0.375	2.251	1353	0.108
0.25	2.143	852	0.117
0.25	2.191	928	0.099
0.25	2.180	989	0.097

Table 4.10 Displacements at the peak loads for 2in Mix 1 samples

Simulated Gap (in.)	Bulk Sp. Gr.	Peak Load (lb)	Shear Displacement (in.)
0.5	2.285	1829	0.137
0.5	2.265	1825	0.119
0.5	2.230	1385	0.139
0.375	2.245	1774	0.118
0.375	2.244	1366	0.126
0.375	2.257	1536	0.126
0.25	2.196	1100	0.141
0.25	2.191	1633	0.096
0.25	2.223	1421	0.138

Table 4.11. Displacements at the peak loads for 1.5 in. Mix 2 samples

Simulated Gap (in.)	Bulk Sp. Gr.	Peak Load (lb)	Shear Displacement (in.)
0.5	2.263	2511	0.106
0.5	2.306	2333	0.107
0.5	2.294	2412	0.106
0.375	2.310	2305	0.116
0.375	2.303	2484	0.081
0.375	2.301	2368	0.102
0.25	2.291	2816	0.092
0.25	2.264	2131	0.097
0.25	2.278	2696	0.116

Table 4.12 Displacements at the peak loads for 2 in. Mix 2 samples

Simulated Gap (in)	Bulk Sp. Gr.	Peak Load (lb)	Shear Displacement (in.)
0.5	2.377	3073	0.136
0.5	2.365	3385	0.110
0.5	2.356	3347	0.091
0.375	2.370	3371	0.118
0.375	2.366	3188	0.121
0.375	2.316	3211	0.11
0.25	2.323	3100	0.12
0.25	2.340	3135	0.091
0.25	2.340	3307	0.111

Figures 4.9 and 4.10 show the averaged peak shear load versus the simulated crack width. It can be seen that the ratio of the peak shear load of the HMA mix decreased with an increase of the simulated crack width. In general, the thicker samples had higher peak shear loads as expected.

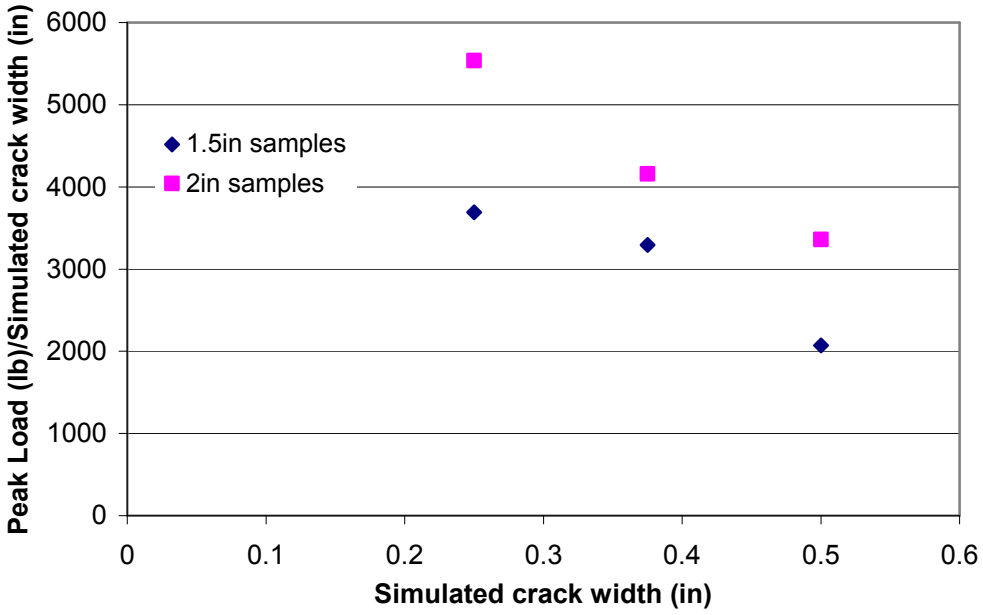

Figure 4.9. Peak shear load versus simulated crack width for Mix 1

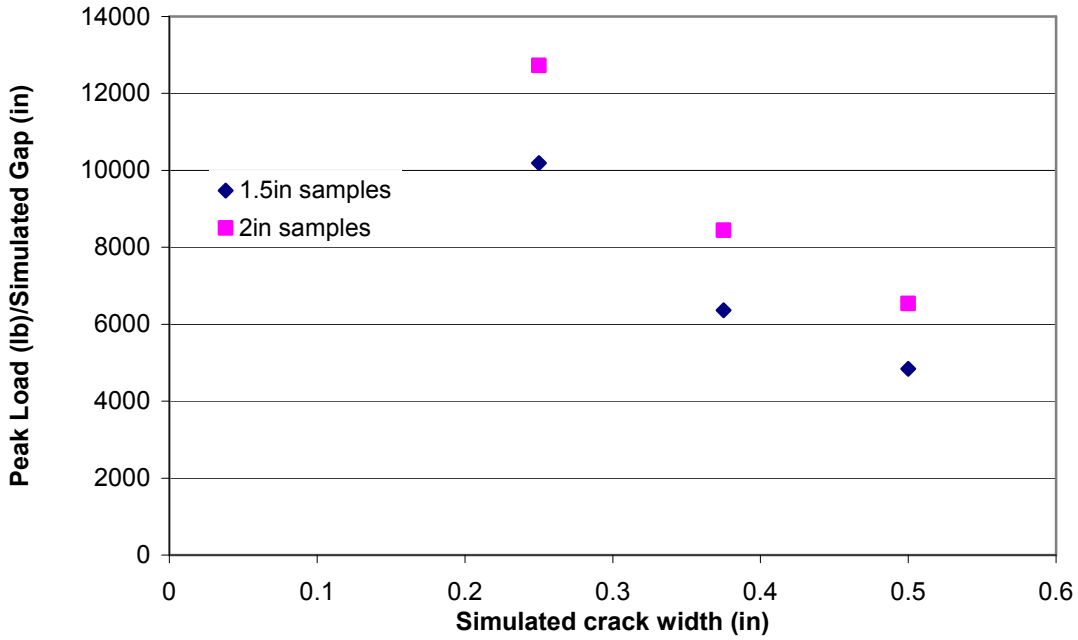

Figure 4.10. Peak shear load versus simulated crack width for Mix 2

Figures 4.11 and 4.12 show the corresponding averaged displacement at the peak load versus the simulated crack width. It can be seen that there is almost no effect of simulated crack width on displacements at peak load**. Figure4.13** shows that the shear displacement at the peak load varied between 4.5 to 9.4 percent of the sample thickness.

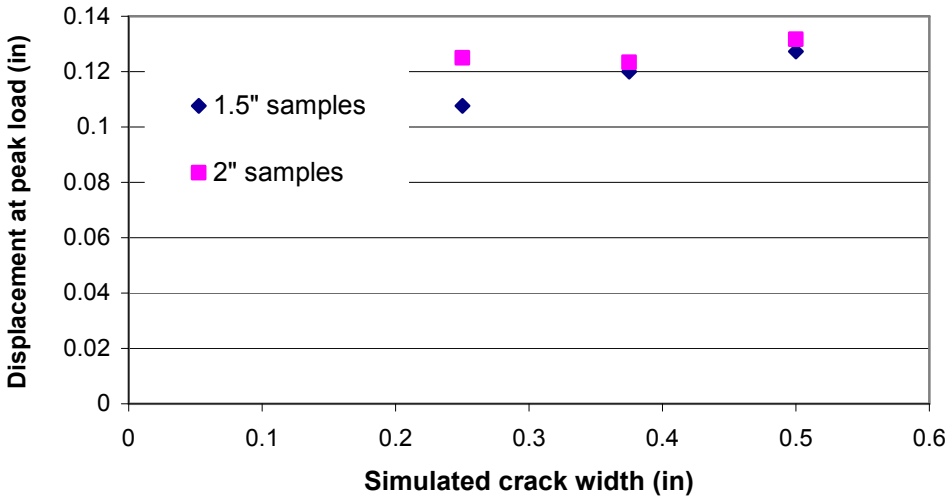

Figure 4.11. Effect of the simulated crack width on the displacement at the peak load for Mix 1

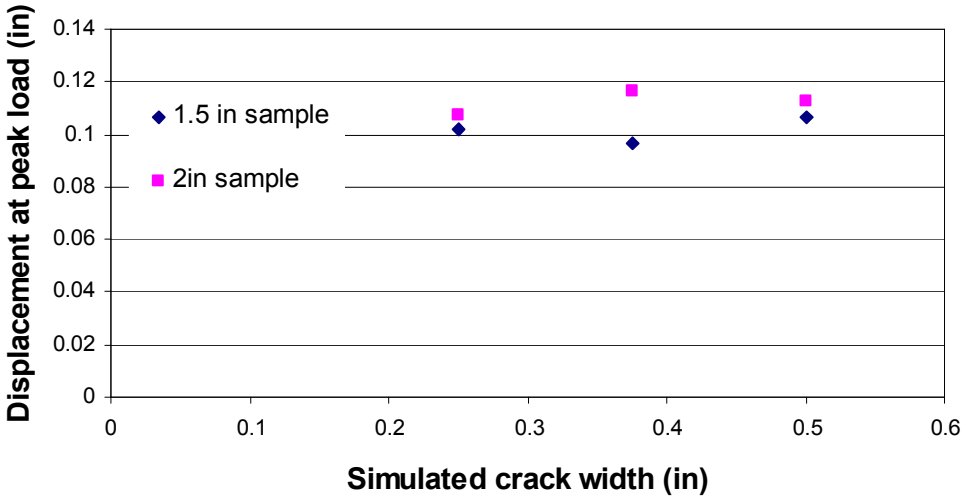

Figure 4.12. Effect of the simulated crack width on the displacement at the peak load for Mix 2

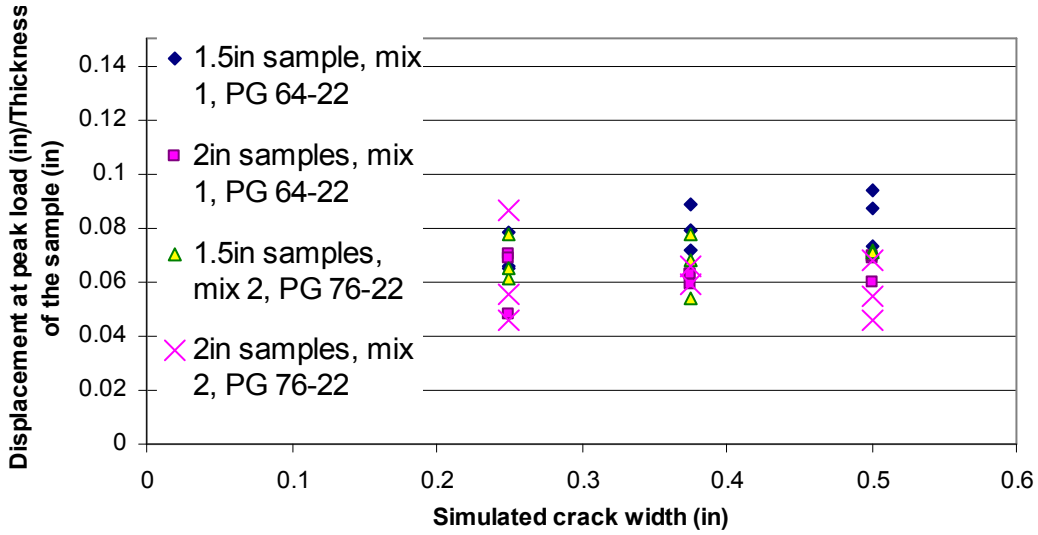

Figure 4.13 Ratio of shear displacement to sample thickness versus simulated crack width

4.2.2 Semi-circular bend test

Knowing the total number of cycles an HMA overlay can endure before failure can help to design or take preventive measurers to minimize the reflection cracking. **Figures 4.14 and 4.15** present the number of cycles before failure of specimens for both Mix 1 and Mix 2 at different levels of loading as compared with the peak static load from the static SCB test. It is shown that an increase of the percentage of the peak static load reduced the number of cycles to failure. For Mix 1, 2 in. thick samples had higher number of cycles than 1.5 in. thick samples. For Mix 2, however, their difference is undistinguishable.

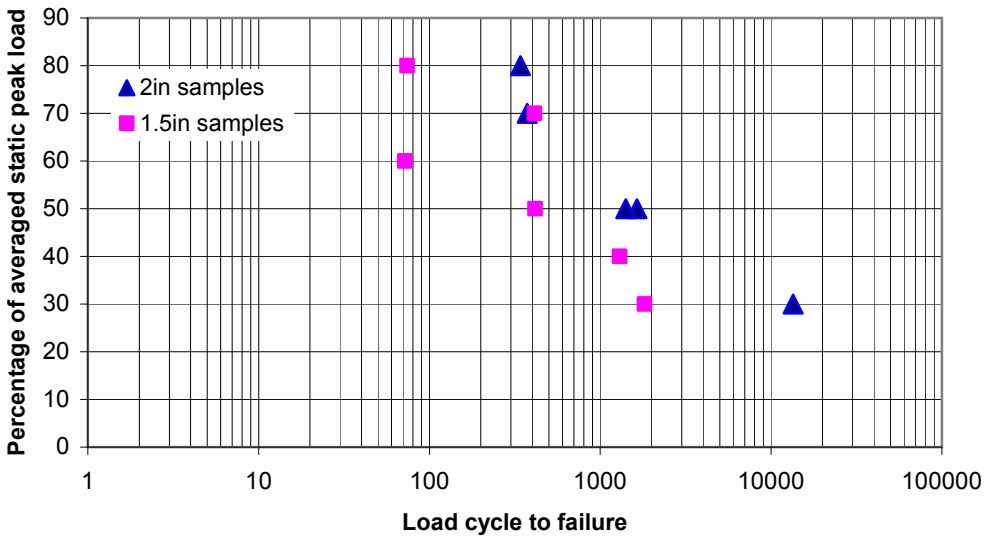

Figure 4.14. Percentage of averaged static peak load versus number of load cycles to failure for Mix 1

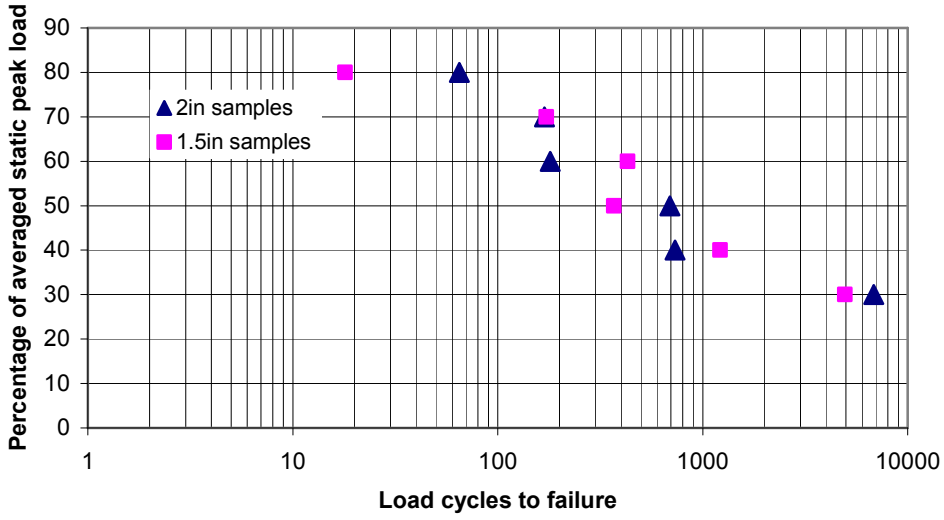

Figure 4.15 Percentage of averaged static peak load versus number of load cycles to failure for Mix 2

Tolerable strain (strain at first crack) is determined by intersection of two straight lines drawn on linear part of strain versus load cycle curve in cyclic semi circular bend test. **Figure 4.16** shows the systematic way of determining tolerable strain of HMA. **Table 4.13** shows the comparison between observed and calculated load cycles to failure.

Figures 4.17 and 4.18 show the relationship between the number of cycles to the first crack of the HMA sample and the static strain at the same load level. In general, the number of cycles to the first crack decreased with an increase in the static strain in the HMA sample except the 2 in. samples for Mix 1.

Table 4.13 Observed and calculated load cycles to first crack

Mix Type	Fraction (%)	Thickness (in)	Observed load cycles to first crack	Calculated load cycles to first crack
1	70	1.5	220	210
1	60	1.5	37	34
1	50	1.5	224	240
1	40	1.5	818	802
1	30	1.5	820	818
1	80	2	296	265
1	70	2	330	215
1	50	2	1258	1133
1	30	2	11170	11095
2	80	1.5	10	10
2	70	1.5	175	173
2	60	1.5	695	431
2	50	1.5	355	369
2	40	1.5	968	1216
2	30	1.5	3848	4951
2	80	2	63	51
2	70	2	140	129
2	60	2	150	165
2	50	2	645	673
2	40	2	673	673
2	30	2	6274	6827

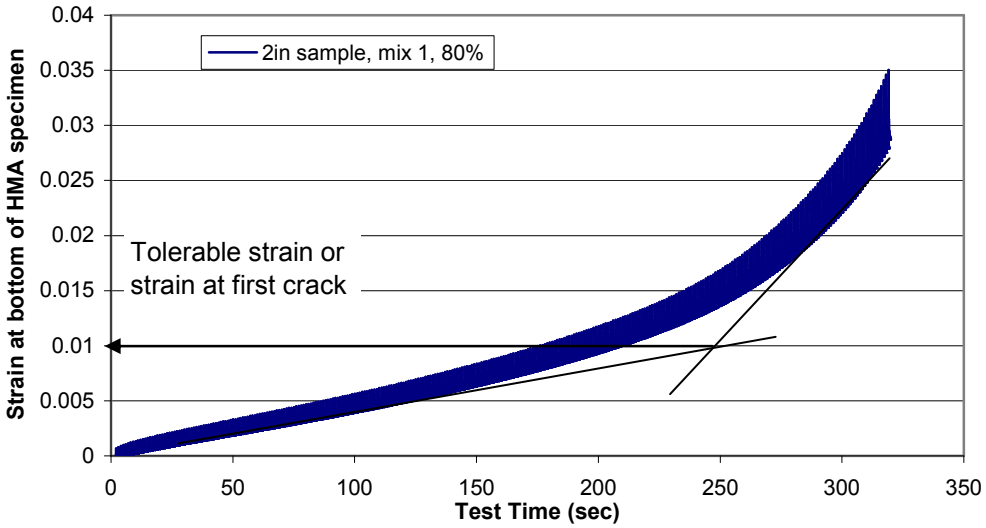

Figure 4.16 Systematic way of determining tolerable strain for HMA mixture

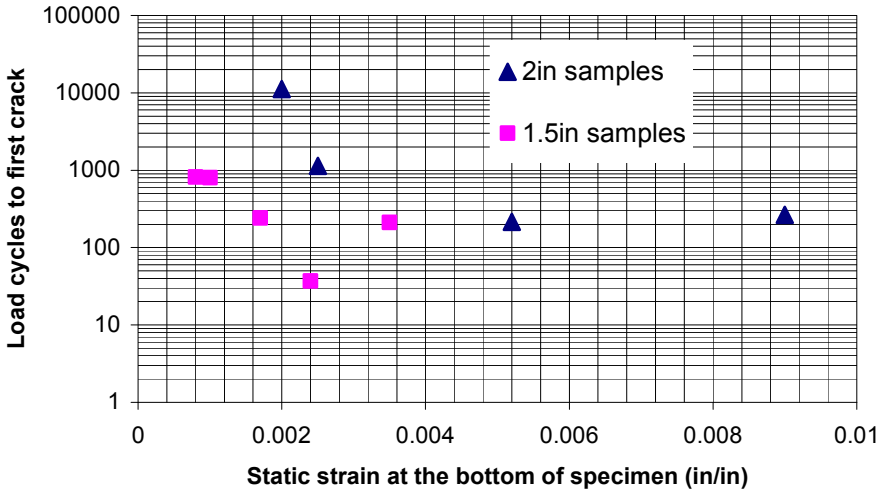

Figure 4.17 Number of load cycles to first crack versus the static strain at the bottom of the HMA specimen for Mix 1

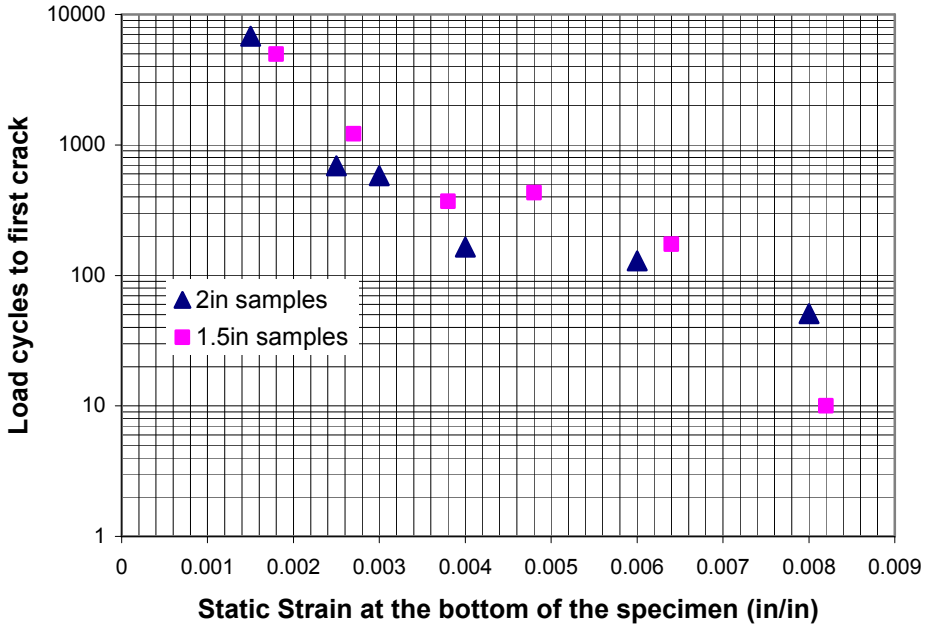

Figure 4.18 Number of load cycles to the first crack versus the static strain at the bottom of the HMA specimen for Mix 2

Figures 4.19 and 4.20 show the relationship between the static strain developed at the bottom of the specimen and the strain developed at the bottom of the specimen when the first crack occurred under cyclic loading. The strain at the bottom of the specimen when the first crack occurred is referred as the tolerable strain. It is shown that the tolerable strain under cyclic loading decreased with an increase of the static strain in the specimen under the same level of loading.

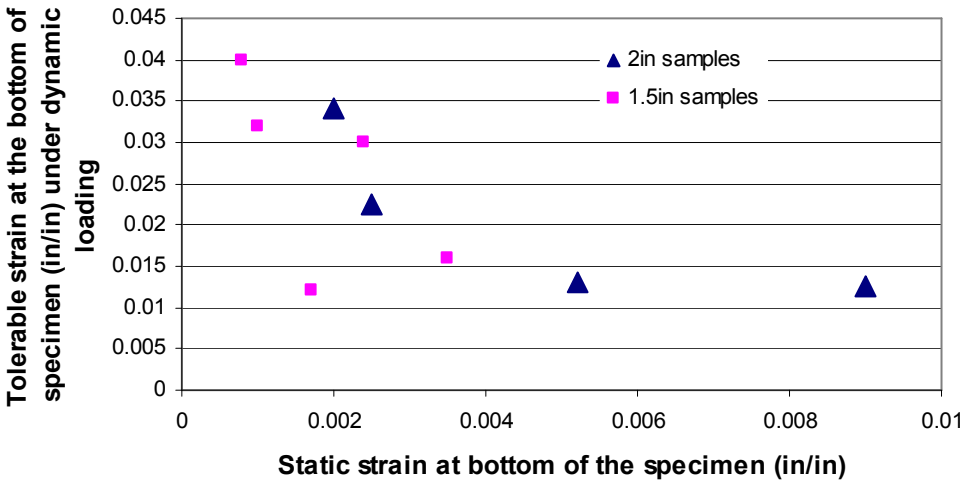

Figure 4.19 Static strain at the bottom of the specimen versus tolerable strain under cyclic loading for Mix 1.

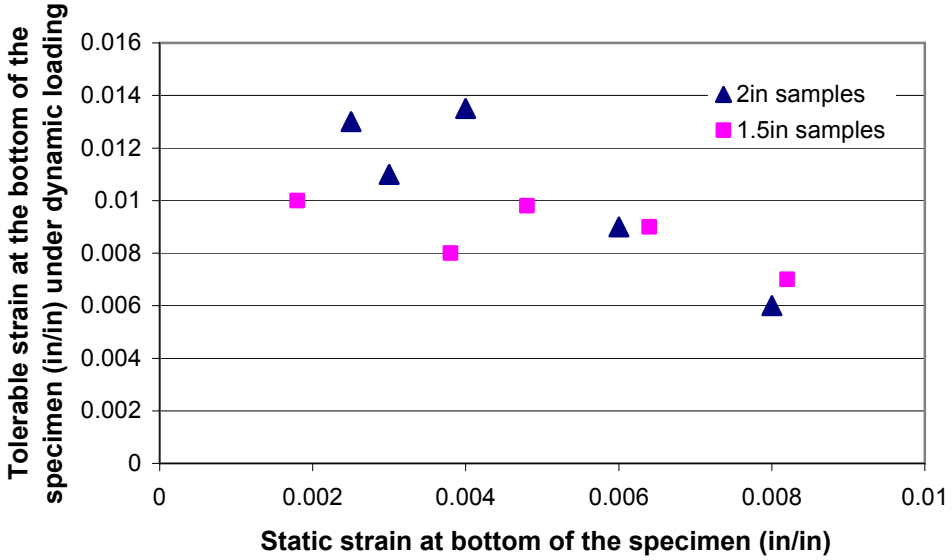

Figure 4.20. Static strain at the bottom of specimen versus tolerable strain under cyclic loading for Mix 2

4.3 Correlation between Static Semi-circular Bend Test and Direct Shear Box Test

Figure 4.21 shows the correlation between the peak compressive load from the static semi-circular bend test and the peak shear load from the direct shear box test. It is shown that the peak compressive load of the HMA obtained from the SCB test is approximately 1.23 times of the peak shear load of the HMA obtained from the direct shear box test.

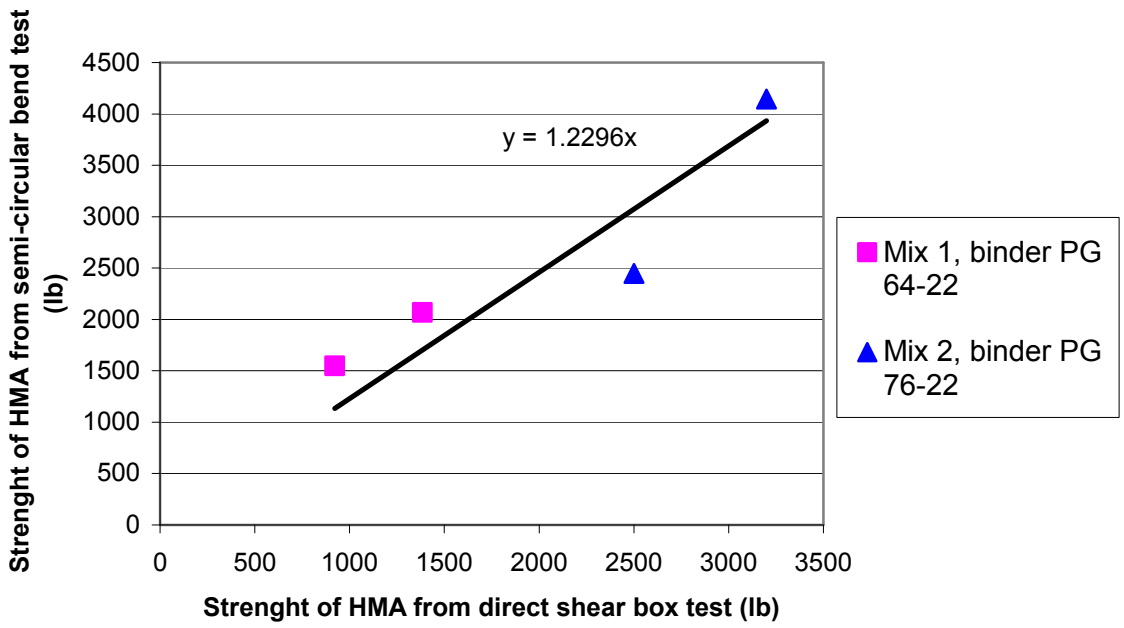

Figure 4.21. Correlation of peak loads between static semi-circular bend tests versus direct shear box tests with crack width 0.25in

5. SUMMARY AND CONCLUSIONS

A laboratory study was conducted to evaluate the shear and tensile characteristics of HMA mixtures chosen from KDOT projects namely 089 C-4318-01 (Mix 1) and 56-29 KA-1087-01 (Mix 2). The shear characteristics were obtained by direct shear box tests while the tensile characteristics were obtained by semi-circular bend tests. Fatigue characteristics were obtained by cyclic semi-circular bend tests. The tolerable strains HMA samples can endure were measured by strain gauges in cyclic semi-circular bend tests. Based on the test results obtained from this study, the following conclusions can be drawn:

- Shear displacement of an HMA sample slightly increases with the simulated crack width. The shear displacement corresponding to the peak shear load varied from 4.5 to 9.4 percent of the sample thickness.
- The simulated crack width had almost slight effect on the peak shear load and displacement at peak load.
- Test results show that semi-circular bend test is an effective method which can characterize the tolerable tensile strains of HMA mixtures. It is shown that Mix 2 is more brittle than mix 1. The tolerable tensile strain for Mix 1 is 3.5 percent and that of Mix 2 is 1.4 percent.
- The peak compressive load of the HMA from the static semi-circular bend test was approximately 1.23 times its peak shear load.

REFERENCES

Abd El-Naby, R.M., Abd El-Aleem, A.M., and S. H. Saber, S.H. (2002) "Evaluation of the shear strength of asphalt concrete mixes: Experimental investigation." Montreal, QB, Canada: Canadian Society for Civil Engineering, pp 2773-2781.

Al-Qadi, I.L., Loulizi, A., Janajreh, I., and Freeman, T.E. (2002) "Pavement response to dual tires and new wide-base tires at same tire pressure," *Transportation Research Record*, No. 1806, pp 38-47.

Arabani, M. and Ferdowsi, B. (2007). “Laboratory evaluating and comparison of Semi-Circular Bend Test results with other common tests for HMA mixtures.” Advanced Characterization of Pavement and Soil Engineering Materials-Loizos, Scarpas and Al-Qadi(eds), Taylor & Francis Group London, ISBN 978-0-145-44882-6, pp. 151-164

Birgisson, B., Soranakom, C., Napier, J.A.L., and Roque, R. (2003) "Simulation of fracture initiation in hot-mix asphalt mixtures," *Transportation Research Record*, No. 1849, pp 183

Brwon, S.F., Thom, N.H., and Sanders, P.J. (2002) “Reinforced asphalt” *Final Report to Tensar International., ABG Ltd., Macafferri Ltd., Scott Wilson Pavement Engineering, Bardon Aggregates, 6D Soilutions., School of Engineering, University of Nottingham, Nottingham, U,K*

Button, J.W. and Lytton, R.L. (2006). “Guidelines for Using Geosynthetics with Hot Mix Asphalt Overlays to Reduce Reflection Cracking.” *Transportation Research Board* Annual Meeting CD ROM

Carpenter, Samuel H., Khalid A. Ghuzlan, and Shihui Shen (2003) "Fatigue Endurance Limit for Highway and Airport Pavements," *Transportation Research Record*, No. 1832, pp 131-138.

Castell, M. A., A. R. Ingraffea, and L. H. Irwin (2000) "Fatigue crack growth in pavements," *Journal of Transportation Engineering*, Vol. 126, No. 4, pp 283-290.

Chen, Xingwei, Baoshan Huang, and Zhihong Xu (2006) "Uniaxial penetration testing for shear resistance of hot-mix asphalt mixtures," *Transportation Research Record*, No. 1970, pp 116-125.

Cortez, E. R and Perkins, S. W., (2005). “Evaluation of Base-Reinforced Pavemets Using Heavy Vehicle Simulator*.” Geosynthetic International, 12, No. 2, pp.86-98*

De Bondt, A.H., (1999) “*Anti-Reflective Cracking Design of Reinforced Asphaltic Overlay*.” Ph.D. dissertation. Delft University of Technology, Netherlands

Ellis, S.J., Langdale., P. C., and Cook J. (2002), “Performance of techniques to minimize reflection cracking and associated development in pavement investigation for maintenance of UK military airfield”. *Presented for the 2002 Federal Aviation Administration Airport Technology Transfer Conference*

Kohler, Erwin, and Jeffery Roesler (2006) "Crack spacing and crack width investigation from experimental CRCP sections," *International Journal of Pavement Engineering*, Vol. 7, No. 4, pp 331-340.

Executive Summary of Technical Presentation made at annual meeting of Association of Asphalt Paving Technology, Savannah, Georgia, March 2006

Francken, L., Vanelstraete, A. and de Bondt, A. H. (1997). “Modelling and structural design of overlay systems.” Vanelstraete, A. and Francken, L., Editors, *RILEM Report 18: Prevention of Reflective Cracking in Pavements*, E & FN Spon, London, 1997, pp. 84–103.

Ghuzlan, K. A., and S. H. Carpenter (2000) "Energy-derived, damage-based failure criterion for fatigue testing," *Transportation Research Record*, No. 1723, pp 141-149.

Huffman, J.E., (1978). “Reflection cracking and control methods.” *Proceeding Canadian Technical Asphalt Association*, Vol. 23.

Huang, B., Li, G. and Mohammand, L.N,(2003) “Analytical Modeling and experimental study of Tensile strength of Asphalt concrete composite at low temperature*.” Composite, Part B: Engineering, Elsevier,* pp 705-714

Huang, Baoshan, Xiang Shu, and Yongjing Tang (2005) "Comparison of Semi-Circular Bending and indirect Tensile strength tests for HMA mixtures." Austin, TX, United states: American Society of Civil Engineers, pp 177-188.

Kim, Seong-Min, Moon C. Won, and B. Frank McCullough (2003) "Mechanistic Modeling of Continuously Reinforced Concrete Pavement," *ACI Structural Journal*, Vol. 100, No. 5, pp 674-682.

Kirschke, K. R., and S. A. Velinsky (1992) "Histogram-based approach for automated pavement-crack sensing," *Journal of Transportation Engineering*, Vol. 118, No. 5, pp 700-710.

Kohler, Erwin R., and Jeffery R. Roesler (2005) "Crack width measurements in continuously reinforced concrete pavements," *Journal of Transportation Engineering*, Vol. 131, No. 9, pp 645-652.

Krans, R.L., Tolman, F., and Van de ven, M.F.C. (1996). “Semi-circular bending test: a practical crack growth test using asphalt concrete cores.” The Third International RILEM Conference, Reflecting Cracking in pavements, Spon Press, UK.

Kumara, M. W., M. Gunaratne, J. J. Lu, and B. Dietrich (2004) "Methodology for random surface-initiated crack growth prediction in asphalt pavements," *Journal of Materials in Civil Engineering*, Vol. 16, No. 2, pp 175-185.

Majidzadeh, Kamran, E. M. Kauffmann, and C. L. Saraf (1971) "Analysis of fatigue of paving mixtures from the fracture mechanics viewpoint," *ASTM Special Technical Publication*, No. 508, pp 67-84.

Masad, E., N. Somadevan, H. U. Bahia, and S. Kose (2001) "Modeling and experimental measurements of strain distribution in asphalt mixes," *Journal of Transportation Engineering*, Vol. 127, No. 6, pp 477-485.

Molenaar, A. A. A. (1993) "Evaluation of pavement structure with emphasis on reflection cracking," *2nd International RILEM conference on reflection cracking*. Laige, Belgium, pp 21-28.

Molenaar, A. A. A., A. Scarpas, X. Liu, and S. M. J. G. Erkens (2002) "Semi-circular bending test; simple but useful?." Colorado Springs, CO, United states: Association of Asphalt Paving Technologist, pp 794-815.

National Asphalt Pavement Association. (1999). “Guidelines for use of HMA overlays to rehabilitate PCC pavement.” *NAPA information series 117.*

Roberts F.L., Kandhal P.S., Brown E.R., Lee D.Y., Kennedy T.W. (1996). “Hot mox asphalt materials, mixture design, and construction*”. Lanham, Maryland: NAPA Education Foundation.*

Selezneva, Olga, Michael Darter, Dan Zollinger, and Samir Shoukry (2003) "Characterization of Transverse Cracking Spatial Variability: Use of Long-Term Pavement Performance Data for Continuously Reinforced Concrete Pavement Design," *Transportation Research Record*, No. 1849, pp 147-155.

Sherman, George (1982) "MNIMIZING REFLECTION CRACKING OF PAVEMENT OVERLAYS," *National Cooperative Highway Research Program, Synthesis of Highway Practice*.

Shen, Shihui, and Samuel H. Carpenter (2005) "Application of the dissipated energy concept in fatigue endurance limit testing," *Transportation Research Record*, No. 1929, pp 165-173.

Sensitivity Evaluation of Field Shear Test Using Improved Protocol and Indirect Tension Strength Test*, NCHRP Web Document 56 (Project 9-18[1]): Contractor's Final Report*.2003

Song, Seong Hyeok, Glaucio H. Paulino, and William G. Buttlar (2006) "Simulation of crack propagation in asphalt concrete using an intrinsic cohesive zone model," *Journal of Engineering Mechanics*, Vol. 132, No. 11, pp 1215-1223.

Wang, H.N., X.J. Liu, and P.W. Hao (2008) "Evaluating the shear resistance of Hot Mix Asphalt by Direct Shear Test," *Journal of testing and evaluation*, Vol. 36, No. 6, p 7.

Wang, Linbing, Laureano R. Hoyos, Louay Mohammad, and Chris Abadie (2006) "Characterization of asphalt concrete by multi-stage true triaxial testing." Tampa, FL, United states: American Society for Testing and Materials, pp 198-207.

Appendix:

1) **Data for material characterization**
2) **Picture of failed samples**
3) **Data for direct shear box test**
4) **Date for Semi-circular bend test**
    a) **Static SCB Test**
    b) **Cyclic SCB Test.**